Plasmofluidics for Biosensing and Medical Diagnostics

5

Xiaolei Peng, Bharath Bangalore Rajeeva, Daniel Teal, and Yuebing Zheng

Contents

X. Peng · B. B. Rajeeva
Materials Science and Engineering Program and Texas Materials Institute, The University of Texas at Austin, Austin, TX, USA

D. Teal
Department of Mechanical Engineering, Materials Science and Engineering Program, Texas Materials Institute, The University of Texas at Austin, Austin, TX, USA

Y. Zheng (✉)
Materials Science and Engineering Program and Texas Materials Institute, The University of Texas at Austin, Austin, TX, USA

Department of Mechanical Engineering, Materials Science and Engineering Program, Texas Materials Institute, The University of Texas at Austin, Austin, TX, USA
e-mail: zheng@austin.utexas.edu

C. S. S. R. Kumar (ed.), *Nanotechnology Characterization Tools for Biosensing and Medical Diagnosis*, https://doi.org/10.1007/978-3-662-56333-5_5

1 Definition of the Topic

Plasmofluidics, an extension of optofluidics into the nanoscale regime, merges plasmonics and micro-/nanofluidics for highly integrated and multifunctional lab on a chip. In this chapter, we focus on the applications of plasmofluidics in the versatile manipulation and sensing of biological cell, organelles, molecules, and nanoparticles, which underpin advanced biomedical diagnostics.

2 Overview

An improved capability of manipulating and sensing living cells, viruses, bacteria, and molecules (i.e., DNAs, proteins, and drug molecules) is significant for biomedical research and disease diagnostics in global health, primary care, and point-of-care (POC) settings. Conventional diagnostic technologies such as polymerase chain reaction (PCR) and enzyme-linked immunosorbent assay (ELISA) have been established as global gold standards. However, they have mainly been used in developed countries and major cities in developing countries due to their sophisticated instrumentation and complex operation procedures that require specially trained staffs [1, 2]. Therefore, there is still a great need for innovative portable POC devices that can provide effective high-value healthcare to underdeveloped and resource-constrained regions. Herein, we argue how plasmofluidics, a synergistic integration of plasmonics and micro-/nanofluidics, can help address current challenges in portable POC devices as well as fundamental biomedical studies. This book chapter focuses on two correlated areas: plasmofluidic tweezers and biosensors. The first part of this book chapter reviews state-of-the-art plasmofluidic tweezers for versatile manipulations of biological cells, DNAs, and proteins, including the latest strategies for overcoming the inherent drawbacks of plasmonic tweezers. The second part discusses various plasmofluidic biosensors for the detection of nucleic acids, proteins, pathogens, and drug molecules. We highlight the progress made at improving the limit of detection (LOD), response time, and accuracy for analyzing clinical samples.

3 Introduction

Infectious diseases, which are caused by bacterial (e.g., pneumonia), mycobacterial (e.g., tuberculosis), viral (e.g., HIV), fungal (e.g., candidiasis), and parasitic pathogens (e.g., malaria), have considerable impact on global economy, health, and security [1, 2]. For instance, recent years have witnessed large outbreaks of Ebola in Africa and Zika in Central and South America, and there have been serious concerns and heated debates on public health at the global scope. Cancers, which are characterized by the uncontrolled growth and spread of abnormal cells and induced by various factors such as tobacco, infectious organisms, genetic mutations, and immune conditions, are the leading cause of death for much of the US

population [3]. The threats from infectious diseases and cancers become increasingly prevalent due to factors such as changing trends in human and animal migration, increasing urbanization, environmental deterioration, and climate change. Early disease diagnosis and effective treatment have become critical for the clinical regulation and management of infectious diseases and cancers. Convectional disease diagnostics has relied on techniques such as optical microscopy, culture, immunoassays, and nucleic acid amplification [4]. A standard process for disease diagnostics includes the following steps: (a) collection and transport of biological samples such as blood, urine, and tissue swabs from the point of care; (b) analysis of the samples by experienced staffs in a centralized laboratory; and (c) notification of the results to the clinicians and patients. Due to highly frequent access to energy resources like electricity, time-consuming procedures, and need for well-trained personnel, the conventional clinical methods prelude the rapid disease detection and response at the primary care. Their drawbacks are prominently revealed in resource-limited and underdeveloped areas.

Point-of-care (POC) devices, which enable on-site test and follow-up action, are promising to improve the diagnosis and management of infectious diseases and cancers in various clinical settings. These include areas where healthcare infrastructure is limited and high-quality timely medical care is inaccessible [5, 6]. With the advancements of nanotechnologies and micro-/nanofluidic technologies, many innovative POC biosensors with optical, electrical, and mechanical interrogations have been developed. However, two major challenges, matrix effect and system integration, have prevented the further developments and uses of POC devices [4]. Most biosensors can have excellent performance with pristine samples. However, they still need to be strictly evaluated with clinical samples due to the matrix effect. Generally, the matrix of human fluids becomes more complex in infected states, which could lead to the clogging of microfluidic channels and the decrease of the transduction signals. Transformation of POC devices from proof-of-concept and benchtop to bedside care and point-of-care settings requires the system integration. However, to integrate and package various modules for sample preparation and signal detection into a fully automated and user-friendly platform remains challenging.

Plasmofluidics, which seeks to synergize plasmonics and micro-/nanofluidics for lab on a chip, is promising for advancing the next-generation POC devices that feature high compactness, high integration, and multiple functions as well as the frontiers of biomedical research [7]. With their capability of controlling light at the nanoscale beyond the diffraction limit, surface plasmons such as surface plasmon polaritons (SPPs) and localized surface plasmon resonances (LSPRs) [8] are effective at optically manipulating, sensing, and analyzing biological cells and molecules [9–11]. Micro-/nanofluidics exploit rich fluidic behaviors at the micro-/nanoscale to enable low-load, high-throughput, cost-effective, and precise delivery of analyte samples. Therefore, plasmofluidic platforms can serve the purpose of processing, sensing, and analyzing biological objects in clinical samples, paving the way toward affordable and portable healthcare devices for their uses in primary care and resource-constrained settings.

There have been several successful review articles on plasmonic biosensing and medical diagnostics [1, 12, 13]. However, a comprehensive review article focused on the emerging field of plasmofluidic sensing is not available yet. To fill the blank, our chapter covers classification, working principles, design strategies, and applications of the state-of-the-art plasmofluidic systems for sensing and medical diagnostics.

4 Experimental Methodology

4.1 Manipulations with Plasmon-Enhanced Optical Near Fields

Biosensing and medical diagnostics often rely on the capability of manipulating biological particles and molecules in fluidic environments. Three prominent techniques that exploit plasmon-enhanced optical near fields to manipulate particles and molecules in fluids have been developed: (i) SPP-based plasmonic tweezers, (ii) LSPR-based plasmonic tweezers, and (iii) plasmonic tweezers based on self-induced back-action (SIBA). Both top-down fabrication techniques such as electron beam lithography and focused ion beam lithography and bottom-up fabrication techniques such as directed assembly and self-assembly have been applied to engineer plasmonic structures for targeted tweezing platforms [14, 15].

SPPs can propagate along the metal-fluid interface with evanescent characteristics perpendicular to the interface. Accordingly, SPP-based tweezers have been used to transport and assemble microscale particles [16–18]. A patterned SPP landscape was constructed from an array of micrometer-sized gold disks on a glass substrate to achieve parallel trapping of individual particles, as shown in Fig. 5.1a [19]. The simulated trapping potential in Fig. 5.1b shows that the trapped particle on the gold disk is stabilized in a forward position along the SPP propagation direction.

Due to the localized electromagnetic fields associated with the excitation of LSPRs, LSPR-based tweezers are often applied to trap single or multiple particles near the plasmonic structures. Plasmonic nanoantennas such as nanodot pairs [20], diabolo structures [21], and bowtie structures [22] were commonly used to induce strong near-field confinement and enhancement in the nanoscale dielectric gaps known as “Hot spots,” which provide stable trapping of nanoparticles at low optical power. Trapping stiffness was enhanced by two orders of magnitude with a metal nanodot pair in a conventional optical tweezers setup, as shown in Fig. 5.1c–d [20]. Despite the localized nature of LSPRs, recent research efforts have achieved long-range transportation of particles by using arrays of plasmonic C-shaped engravings [23] and gold nanoislands with a network of “hot spots” [24].

LSPR-based tweezers exhibit limits in manipulating particles that are smaller than 100 nm due to the high-power requirement and significant thermal effects. SIBA-based plasmonic tweezers were developed to reduce the required power intensity by more than an order of magnitude [25]. As illustrated in Fig. 5.1e, a nanoaperture redshifts in its resonance wavelength when the trapped particle has a larger refractive index than solvent, enhancing the laser beam transmission through the nanoaperture. When the particle tends to escape from the aperture, a drop in the light transmission

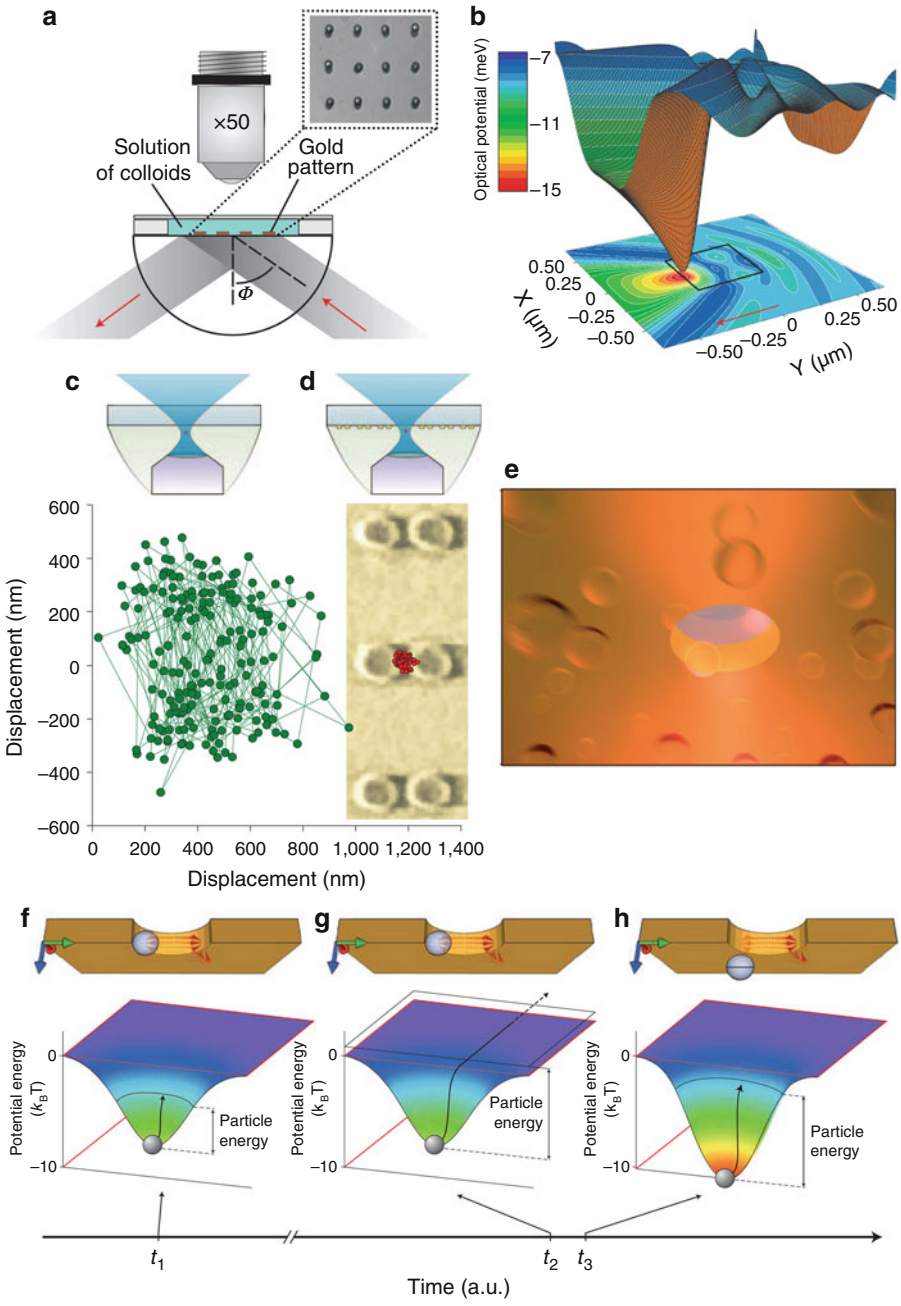

Fig. 5.1 Plasmonic tweezers based on plasmon-enhanced optical near fields. (**a**) Experimental demonstration and (**b**) simulated optical potential for parallel trapping of particles with SPP-based tweezers. Reproduced with permission [19] (Copyright 2007 Nature Publishing Group). (**c**) and (**d**)

generates a restoring force and pulls the particle back to the equilibrium position. In other words, when the particle is moving away from the optical potential well, the SIBA force will deepen the potential well and maintain the trapping state, as illustrated in Fig. 5.1f–h.

4.2 Manipulations with Plasmon-Enhanced Photothermal Effects

Along with the enhanced electromagnetic fields, surface plasmons can induce strong light absorption and photothermal effects [26]. The competing factors between light absorption and heat dissipation determine the temperature increase and spatial temperature distribution. For a spherical gold nanoparticle immersed in water and illuminated by a laser of LSPR wavelength, the temperature increase is uniform in the particle and inversely proportional to the distance outside the particle, resulting in a thermal gradient built up at the metal-water interface [26]. For metal nanoparticle arrays as illustrated in Fig. 5.2a, two heating regimes exist depending on the particle size, particle number, and geometry of the array. These are temperature confinement regime and temperature delocalization regime, as shown in Fig. 5.2b [27]. To reach the temperature confinement regime, both large spacing between nanoparticles and small illumination area are preferred.

The plasmon-assisted heating was exploited to control fluid motion at the microscale and nanoscale [28]. In typical plasmofluidic systems where the characteristic size of the plasmonic structure is very small (~100 nm), thermal diffusion of the fluid dominates in heat dissipation and thermal convection plays a minor role. As shown in Fig. 5.2c–d, the thermal convection velocity at small plasmonic structures is limited to 1–100 nm/s. In this case, the thermal convection can barely contribute to the motion of the particles in the fluidic environment. The thermal convection field can be further damped by more than one order of magnitude when the height of the fluid chamber is reduced to ~10 μm, as illustrated in Fig. 5.2e.

4.3 Plasmonic Sensing of Particles and Molecules

Optofluidic biosensing platforms based on surface plasmons have advantages of being highly integrated, miniaturized, and sensitive. SPP-based sensors typically

Fig. 5.1 (continued) Schematic illustrations of optical setup and time-resolved tracking of a bead trapped by a highly focused laser beam above a glass substrate without and with gold nanodot pairs, respectively (Reproduced with permission [20]. Copyright 2008 Nature Publishing Group). (**e**) Schematic illustration of the trapping of a single PS bead within an aperture in a thick gold film based on the SIBA mechanism (Reproduced with permission [25]. Copyright 2009 Nature Publishing Group). (**f**–**h**) Schematic illustration, together with simulated optical potential, for the working principle of SIBA-based tweezers (Reproduced with permission [10]. Copyright 2011 Nature Publishing Group)

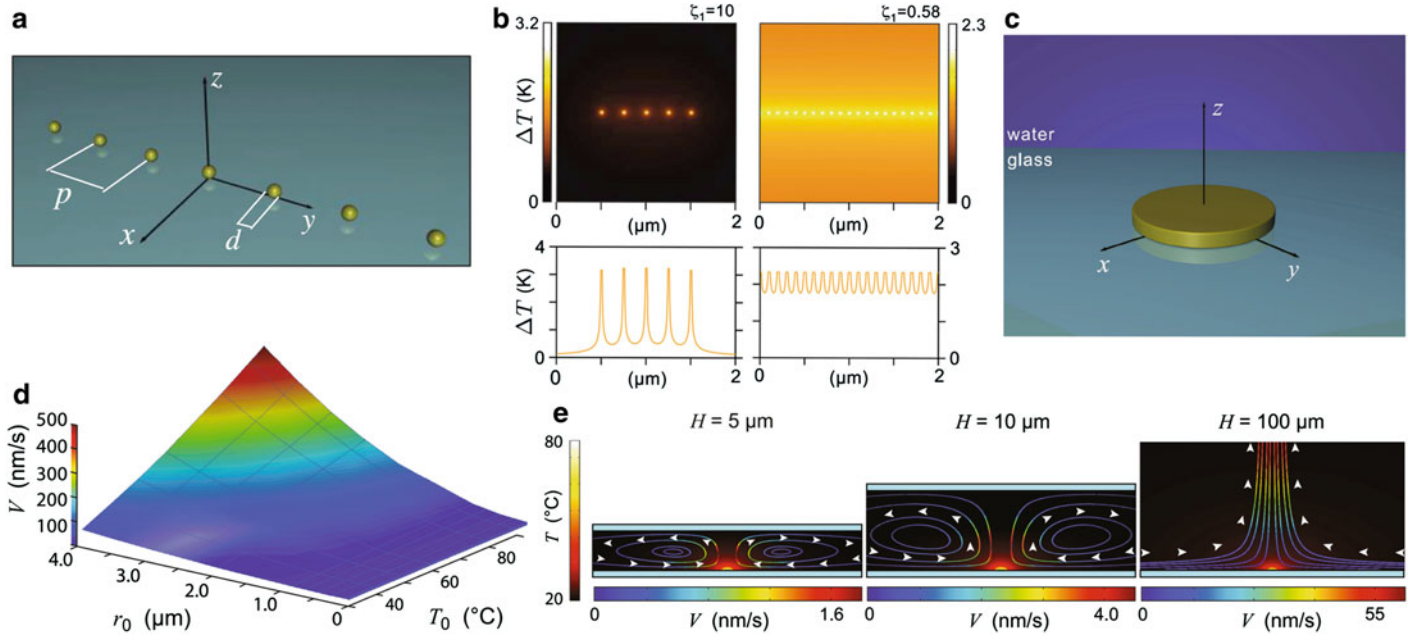

Fig. 5.2 Manipulations in fluids with plasmon-enhanced photothermal effects. (**a**) Schematic representation of a chain of gold nanoparticles on a glass substrate that is immersed in water. (**b**) Comparison of temperature confinement regime and temperature delocalization regime (Reproduced with permission [27]. Copyright 2013 American Chemical Society). (**c**) Schematic representation of a gold disk on a glass substrate that is immersed in water. (**d**) Thermal convection velocity magnitude as a function of the disk temperature and the disk radius in (**c**). (**e**) Thermal convection velocity profile as a function of the fluid chamber height (Reproduced with permission [28]. Copyright 2011 American Chemical Society)

interrogate the change in resonance angle in attenuated total internal reflection to detect target specimens and to extract binding kinetics, as shown in Fig. 5.3a [1, 29]. The specimen-binding events change the dielectric constant over the metal layer. Several approaches have been applied to excite SPPs, including prism coupling [30, 31], grating coupling [32], and waveguide coupling [33]. LSPR-based sensors utilize the strong electromagnetic response of metal nanoparticles to refractive-index changes in their surroundings [1, 12, 34, 35]. Various nanostructured metal arrays such as nanohole arrays [36, 37], nanowell arrays [38], nanocross arrays [39], nanocube arrays [40], nanomouth arrays [41], nanomushroom arrays [42], nanodisk arrays [15, 43], and nanobowtie arrays [44] have been designed for the refractive-index sensing with high figure of merit (FOM). Various techniques such as focused ion beam lithography, electron beam lithography, soft lithography, and nanosphere lithography have been employed to fabricate the large-scale arrays with good repeatability [34, 45–47].

Of particular interest are metal nanohole arrays integrated with complex fluidic structures for versatile and parallel sensing [48, 49]. On-chip nanohole array-based sensors feature simple optical instrument and high synergy with microfluidic schemes. In the flow-over mode (Fig. 5.3b), only the upper metal surfaces of the nanohole arrays are exploited like those in the convectional SPP-based sensors. Through scaling analysis and numerical simulation, Escobedo's group has found that the flow-through mode features ~10-fold enhancement of time response over the flow-over mode in typical biosensing applications [36]. Further experiments showed that the flow-through mode enabled active delivery, concentration, and sensing of analytes, leading to one order of magnitude increase in sensing efficiency and two orders of magnitude improvement in LOD [37].

In general, a LSPR biosensor consists of the following components: (i) a recognition element in conjunction with the plasmonic substrate, (ii) a transducer to convert the interaction between target and recognition element to optical or electrochemical output signals, and (iii) a system to interrogate the signals. Spectroscopic measurements are the most common approach for the signal analysis, which include (i) transmission spectroscopy (Fig. 5.3c), (ii) reflection spectroscopy (Fig. 5.3d), and (iii) dark-field scattering spectroscopy (Fig. 5.3e) [50]. Surface plasmon resonance imaging (SPRI) has been developed to perform large-area measurements at high resolution [51]. It is a label-free method of visualizing binding activities across an arrayed biochip via a video CCD camera.

Surface-enhanced Raman spectroscopy (SERS), which often arises from the strong electromagnetic field enhancement proximate to the metal surface, has proved as a powerful tool for label-free analysis of molecules. SERS interrogates Raman shifts originating from molecular vibrational energy levels [53–55]. Metal colloids, colloid aggregations in solutions, and metal nanoparticle arrays on substrates are commonly used for SERS-active sensors integrated with microfluidics [55, 56]. There are two major microfluidic approaches toward SERS-active plasmofluidic sensors: (i) mixing the sample with SERS-active colloids in a microfluidic channel

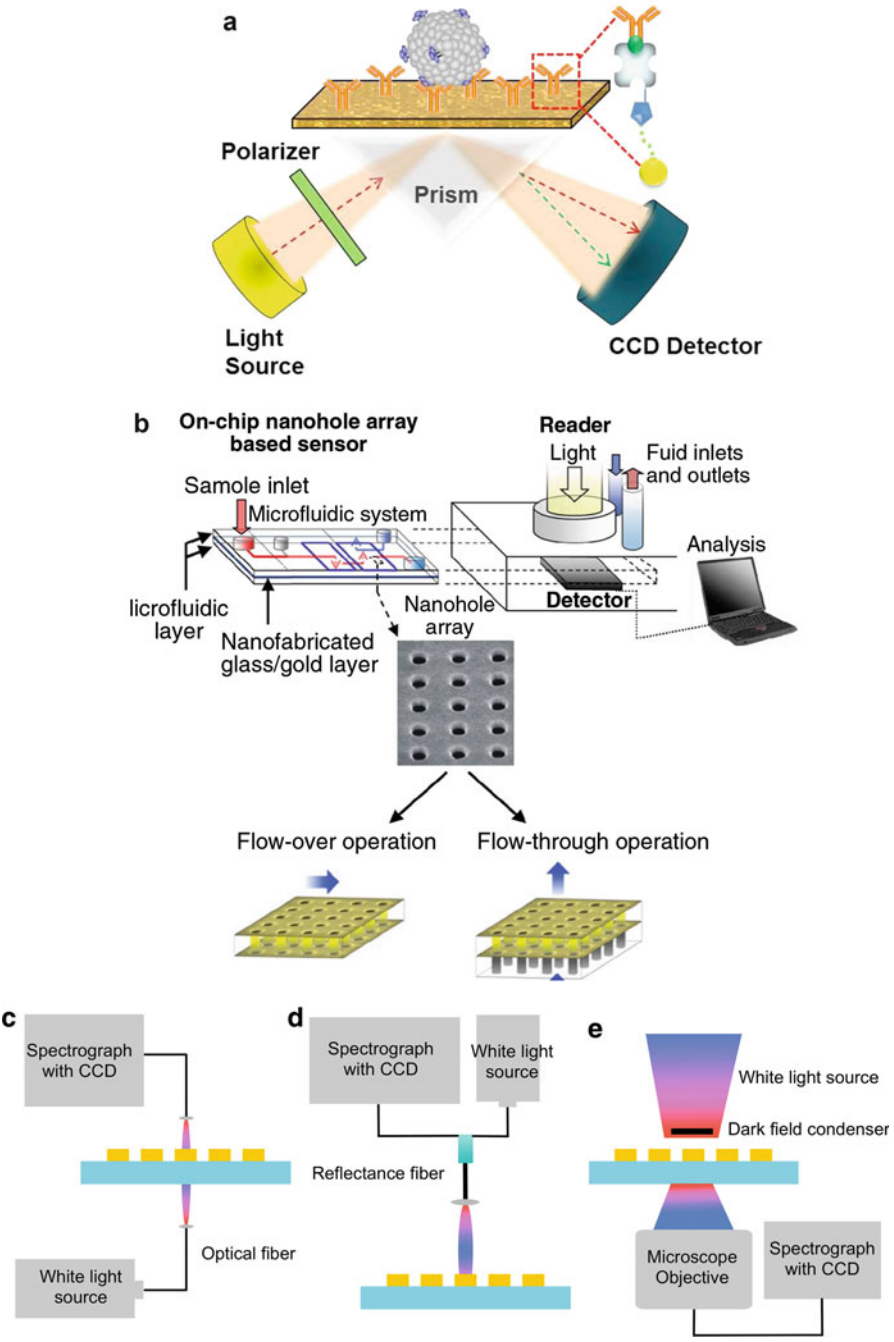

Fig. 5.3 (continued)

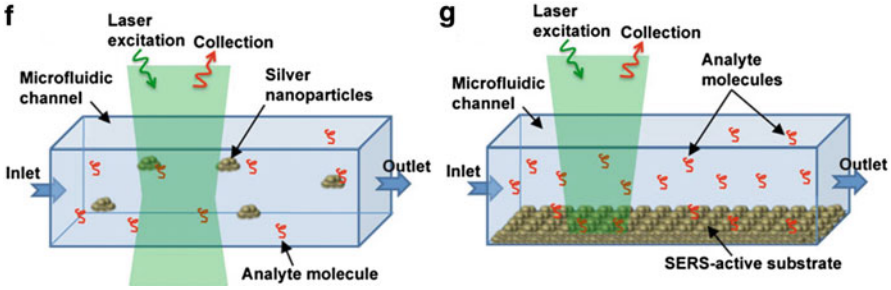

Fig. 5.3 Plasmonic sensing of biological particles and molecules. (**a**) Schematic depiction of a SPP-based sensor in the Kretschmann configuration. The metal surface is functionalized with recognition elements for selective detection. Once biological particles or molecules are captured by the metal surface, the SPP mode will be modified, and a signature in the reflected light will be probed by a detector for analysis (Reproduced with permission [1]. Copyright 2015 American Chemical Society). (**b**) Schematic depiction of an on-chip LSPR sensing platform based on metal nanohole arrays. The fluid can be transported over or through the nanoholes. The platform also includes external components such as a light source, a detector, and a fluidic actuator (Reproduced with permission [48]. Copyright 2013 RSC Publishing). Schematics of the instrumental setups for LSPR sensing that perform optical (**e**) transmission, (**f**) reflection, and (**g**) scattering measurements. (**f**–**g**) Schematic depictions of SERS-based on-chip sensors integrated with microfluidics. (**f**) Mixed solution of analytes and nanoparticles is driven through a microfluidic channel that is under laser illumination and Raman recording. (**g**) Analyte solution is driven through a microfluidic channel with a SERS-active substrate at the bottom of the channel (Reproduced with permission [52]. Copyright 2012 Springer Publishing)

(Fig. 5.3c) and (ii) driving the sample through a microfluidic channel with a SERS-active substrate at the bottom (Fig. 5.3d) [52]. Such plasmofluidic sensors have the advantages of measuring biological particles and molecules in their native watery environments. However, since the molecular adsorption or binding to the SERS-active surfaces relies on the diffusion of the analytes in solutions, the Raman signal intensities will be weaker than those of SERS based on dried samples on solid-state Raman substrates.

Various active and passive concentration techniques have been developed to improve the SERS LOD in fluidic systems [52]. Recently, we have developed a technique that uses plasmon-enhanced thermophoresis for reversible and dynamic assembly of plasmonic nanoparticles for in situ SERS analysis of molecules, as shown in Fig. 5.4a [57]. Once a temperature gradient is created on a plasmonic substrate that is illuminated with a low-power laser beam, the positive-charged nanoparticles will migrate to the hot region under a thermally induced local electrical field (Fig. 5.4b) and form nanoparticle assemblies at the laser spot (Fig. 5.4c). As shown in Fig. 5.4d, the dynamic assemblies feature a high particle density and small interparticle distance, which are suitable for the excitation of multiple electromagnetic "hot spots" for SERS with enhanced sensitivity.

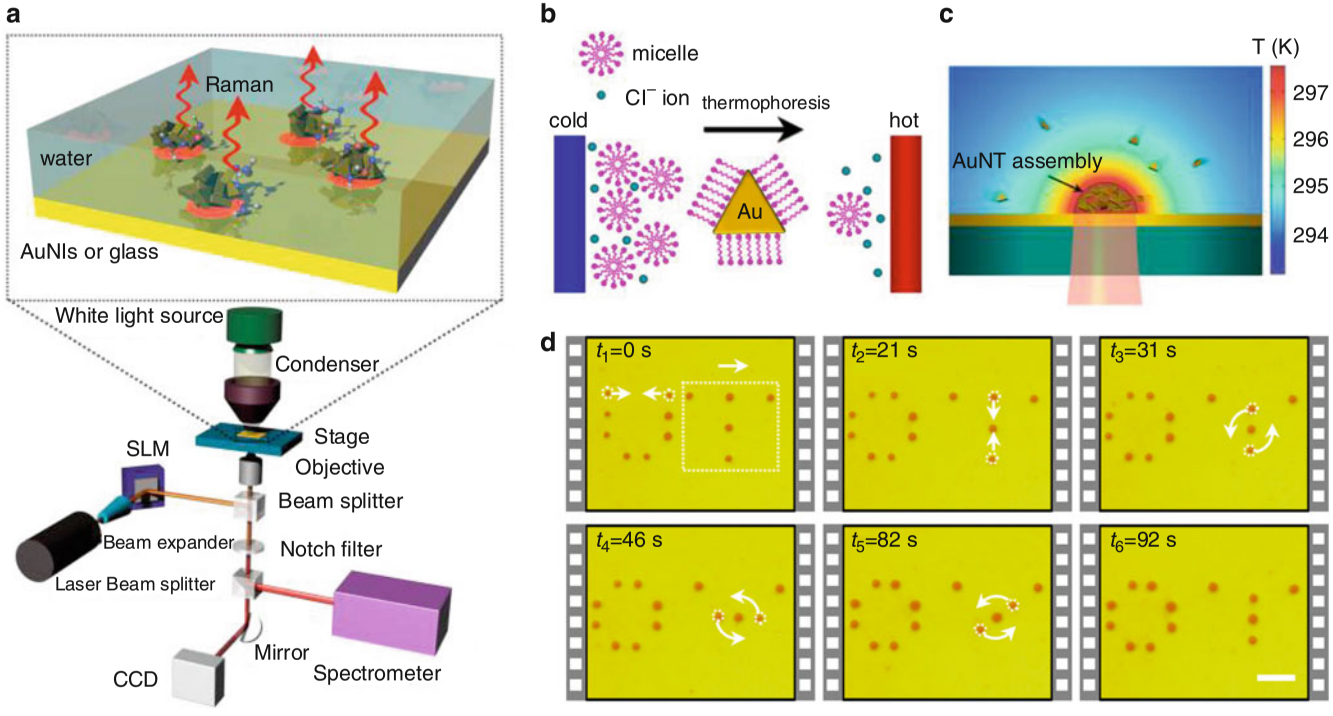

Fig. 5.4 Nanoparticle assemblies by plasmon-enhanced thermophoresis for SERS-based sensing in liquid environments. (**a**) Schematic illustration of the experimental setup for nanoparticle assembly and in situ SERS. (**b**) Migration and (**c**) assembly of positively charged metal nanoparticles in a plasmon-enhanced temperature gradient field. (**d**) Time-evolved optical images of dynamic manipulation of multiple nanoparticle assemblies (Reproduced with permission [57]. Copyright 2016 American Chemical Society)

5 Key Research Findings

5.1 Versatile Manipulations of Particles and Molecules in Plasmofluidic Systems

Manipulations of biological particles and molecules such as trapping, immobilization, and pre-concentration are becoming a critical component of biosensing and analysis in fluidic environments. Plasmonic tweezers have been employed in manipulating various bio-specimens such as cells [58, 59], DNAs [60, 61], and proteins [62–64] at high spatial resolution and low optical power. Using simple optics to create the trapping force, plasmonic tweezers can be readily incorporated into microfluidic systems to design novel plasmofluidic chips with functionalities such as single-particle trapping [57, 62], parallel trapping [58], co-trapping [63], and kinetic detection of biological objects [61, 64]. One has also recognized multiple issues of current plasmofluidic systems and proposed new solutions. First, due to the near-field nature of surface plasmons and weak thermoplasmonic convection, only particles that diffuse to the close proximity to the plasmonic structures can be captured [65]. Second, isolated plasmonic nanostructures are commonly used to avoid collective heating and particle agglomeration, preventing long-distance transportation and dynamic manipulations. Third, in contrast to conventional optical tweezers that are capable of three-dimensional (3D) manipulations, plasmonic tweezers are often limited to two-dimensional (2D) trapping of objects at the plasmonic structures. New solutions to these issues in the plasmofluidic systems include the adoption of optical components with a higher level of spatial control [66] and the exploitation of loss-induced heating at the plasmonic structures [67].

5.1.1 Plasmon-Enhanced Trapping of Single Biological Cells and Molecules

The capability of trapping fragile biological objects such as cells, DNAs, and proteins in fluids is of significant importance in cellular and molecular biotechnology. *E. coli* cells were trapped in parallel with near-infrared LSPRs on the arrays of plasmonic nanoantennas in a Kretschmann optical setup [58]. The cells were stably aligned along the antennas' long axis, and their continuous growth and division were kept over 2 h. There was no difference in the average division time between the optically trapped cells and those outside the illuminated region. In contrast, optical tweezers have challenges in trapping the *E. coli* cells for their low refraction index (1.38 for visible light) and small dimensions ($2 \times 0.8\ \mu m^2$ at infant stage).

We invented opto-thermophoretic tweezers that can achieve light-directed versatile manipulations of biological cells at an optical power 100–1000 times lower than that of optical tweezers, as illustrated in Fig. 5.5a [68]. By harnessing the permittivity gradient in the electric double layer of the charged surface of the cell membrane, we succeeded at the low-power cell trapping with a plasmon-enhanced temperature gradient field. Arbitrary spatial arrangements of cells at a resolution of ~100 nm and precise rotation of both single and multiple cells were demonstrated with an optical control system based on a digital micromirror device (DMD).

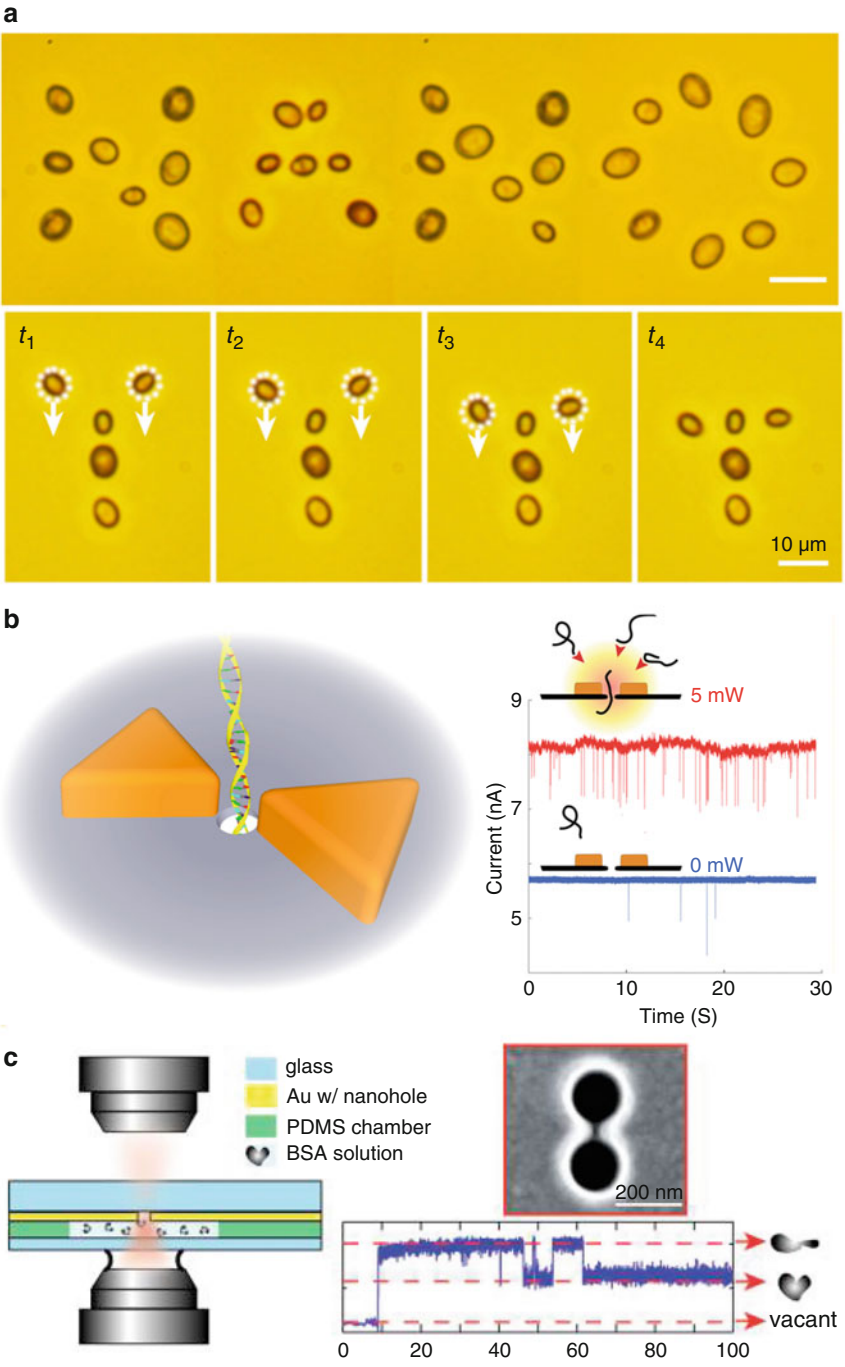

Fig. 5.5 (continued)

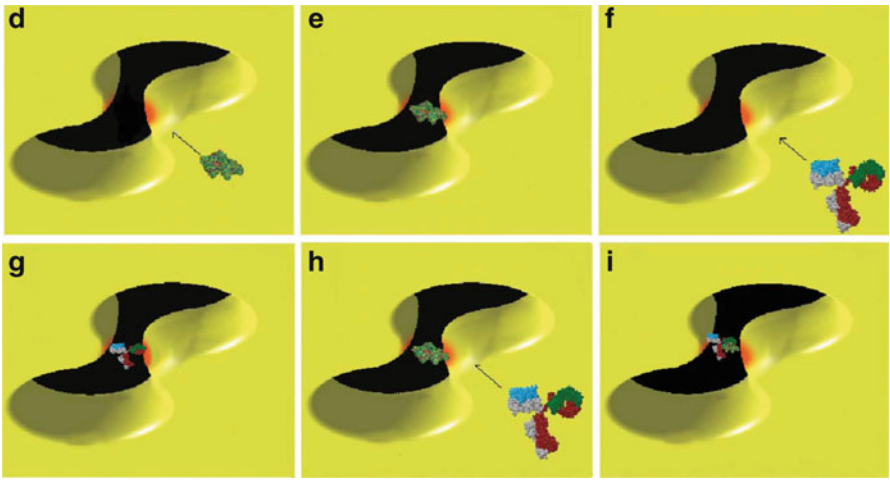

Fig. 5.5 Plasmon-enhanced trapping of biological cells, DNAs, and proteins in fluidic environments. (**a**) Parallel and dynamic trapping of yeast cells with plasmon-enhanced thermophoretic tweezers (Reproduced with permission [68]. Copyright 2017 American Chemical Society). (**b**) Trapping of single DNAs and enhancement of DNA translocation events with plasmonic excitation. The DNA translocation events are characterized by measuring the time-resolved open-pore current traces (Reproduced with permission [61]. Copyright 2014 American Chemical Society). (**c**) Two capture states and the vacant state of single-protein manipulation at the plasmonic "hot spot" of a gold double nanohole. The trapping states of the protein are monitored with time traces of the optical transmission through the double nanohole (Reproduced with permission [62]. Copyright 2011 American Chemical Society). (**d**–**i**) Schematic illustration of the co-trapping process for a BSA molecule and an anti-BSA molecule at the plasmonic "hot spot" of the double nanohole (Reproduced with permission [63]. Copyright 2013 RSC Publishing)

Optical trapping of single DNA molecules and DNA translocations in LiCl buffers were demonstrated using a solid-state plasmonic nanopore, as shown in Fig. 5.5b [61]. The nanopore is positioned between the gap of a gold bowtie antenna. The enhancement of the rate of DNA translocation events was observed and attributed to the plasmon-assisted local heating and the thermophoresis in the thermal gradient. In another example, single bovine serum albumin (BSA) molecules were trapped onto a double-hole structure with a 3.5-mW laser beam focused by a 100× oil immersion objective [62], as shown in Fig. 5.5c. The folding and unfolding states of a trapped BSA molecule were revealed by measuring the intensity of the transmitted light. The same research group demonstrated the protein-antibody co-trapping at the double-hole structure and measured the binding kinetics of the protein-ligand interaction, opening up new avenues for studying intermolecular interactions at the single-molecule level [63, 64].

5.1.2 Three-Dimensional Manipulations and Long-Range Transportation of Objects

"Ideal" tweezers for biological samples in fluidic environments should be able to rapidly deliver target objects and to achieve high-resolution 3D trapping at any

desired locations. To realize 3D low-power trapping and transportation of sub-100-nm objects over a long range, Quidant's group implemented the SIBA-based tweezers at the tip extremity of a metal-coated optical fiber, which can be raster-scanned in all three spatial directions for dynamic manipulations and simultaneously used to collect the reflected signal and identify the different trapping regimes [66], as shown in Fig. 5.6a–b. The optical-fiber-based plasmonic tweezers are attractive for in vivo applications, such as trapping proteins or viruses of interest in cells.

To solve the long-standing challenge of rapid and on-demand loading of objects at the plasmonic trapping sites, Boltasseva's group has combined the plasmonic heating and AC electrical fields for fast delivery and trapping of nanoobjects within a few seconds [65]. The coupling of the plasmon-enhanced temperature gradient and an applied AC electrical field induces an electrothermoplasmonic (ETP) flow, which leads to fluidic motion two orders of magnitude faster than the thermoplasmonic convection and greatly increases the particle capture efficiency, as shown in Fig. 5.6c–d. With their capability of rapid manipulation and concentration of DNA and protein samples, the hybrid plasmofluidic tweezers can be applied for nanoscale biosensors to improve the sensing throughput and efficiency.

5.2 High-Performance Sensing, Analysis, and Diagnostics in Plasmofluidic Systems

Benefiting from a synergy between plasmonic nanotechnology and micro-/nanofluidics, biosensors based on plasmofluidic platforms are attractive for POC devices [1, 2, 7]. They have been applied for portable sensing, analysis, and diagnostics in biomedicine and healthcare. The analytes include nucleic acids, protein, viruses, bacteria, and drugs. Tremendous efforts have been made to improve LOD, response speed, and accuracy of multiplexed identification. More innovative approaches are being developed to push proof-of-concept or benchtop prototypes into practical uses in directly analyzing bio-objects in body fluids for disease diagnosis. Herein, we focus on plasmofluidic POC sensing for DNAs/RNAs, proteins, viruses, bacteria, and drugs.

5.2.1 Detection of DNAs and RNAs

Detection and analysis of DNAs and RNAs are important for disease diagnostics as specific bacteria and viruses in complex samples can be distinguished based on their unique DNA/RNA sequences [2]. Conventional technologies for nucleic acid sensing feature high precision and optimal LOD. However, they require sophisticated instrumentation with multiple time-consuming steps, including pathogen isolation, PCR, and target identification. Plasmofluidic sensors are extensively explored to achieve precise, multiplexed, and label-free detection [31, 69–72]. Springer et al. demonstrated a SPP sensor with a four-channel flow cell (known as dispersionless microfluidics), as shown in Fig. 5.7a–b. The microfluidics suppressed the decrease of analyte concentration at the sensing area when different liquid samples were switched and thus improved the kinetic response and sensitivity [73]. Short

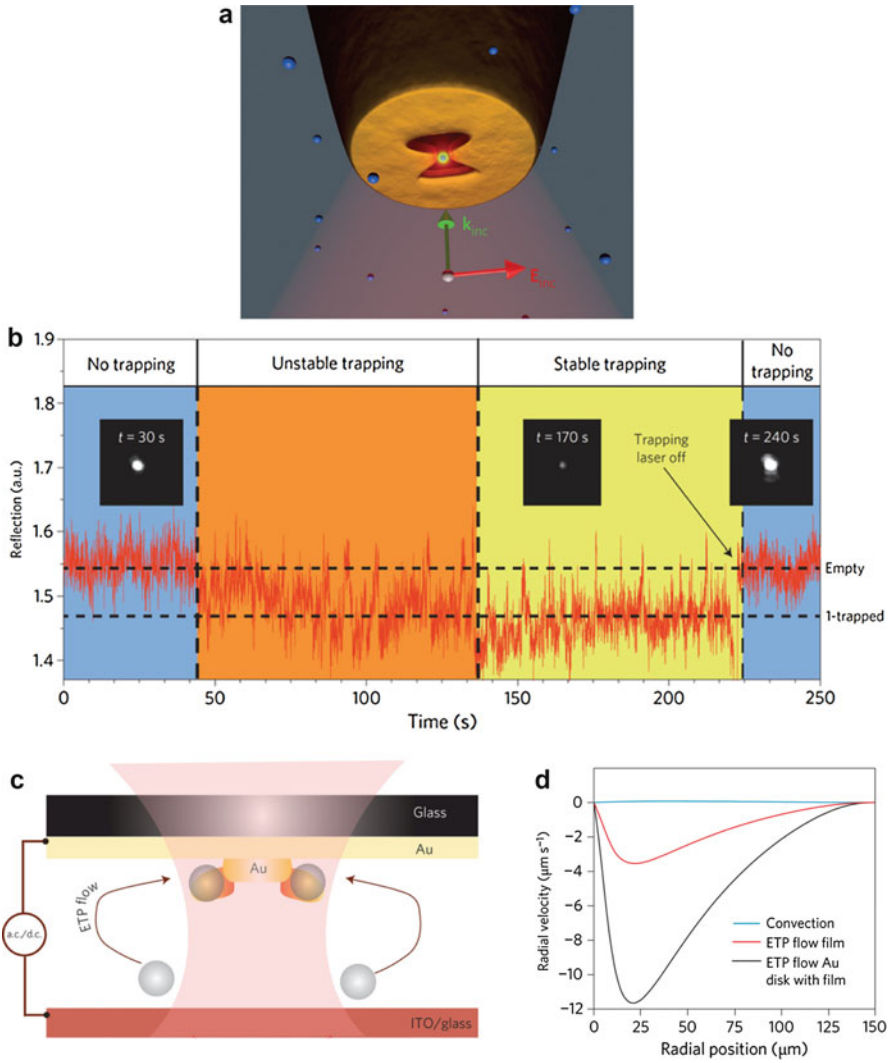

Fig. 5.6 3D manipulation and long-range transportation of objects in plasmofluidic systems. (**a**) Schematic illustration of a single particle trapped at a bowtie plasmonic aperture on the tip of an optical fiber, which is mechanically controlled to enable 3D manipulation of the trapped particle. (**b**) Dynamics of light reflection for different regimes in the 3D manipulation. Insets: Optical images of the light spots at the fiber for the different times as indicated (Reproduced with permission [66]. Copyright 2014 Nature Publishing Group). (**c**) Schematic illustration of hybrid electro-thermoplasmonic (ETP) nanotweezers. The locally heated nanoantenna induces an ETP flow under an AC electric field, which enables rapid and accurate delivery of particles to the trapping site. (**c**) Comparison of radial velocities that result from ETP flow and thermoplasmonic convection as a function of distance from the center of the laser beam (Reproduced with permission [65]. Copyright 2015 Nature Publishing Group)

sequences of DNA (20 bases) that are characteristic for *E. coli* cells were probed in less than 4 min for a concentration down to fM levels, outperforming most SPP sensors by one order of magnitude.

SERS-based plasmofluidic sensors for high-throughput detection of multiple DNAs in single assays were also developed. One example is based on self-assembled gold nanoparticles (Au NPs) on a gold nanowire (Au NW) at the presence of target DNAs [69]. Raman signal was significantly enhanced by placing the DNA molecules in the interstices of the gold-particle-on-wire structure. The structure was constructed by sequential incubation of Au NWs premodified by thiolated probe DNAs in solutions of target DNAs and Au NPs functionalized by reporter DNAs with Raman dyes (Fig. 5.7c). A high selectivity is assured because only those target DNAs with sequences complementary to the probe DNAs and the reporter DNAs can form the particle-on-wire structure for the enhanced signal of the Raman dyes. The sensor was applied for quantitative detection of DNA concentrations, multiplexed detection of bacterial DNAs, and identification of pathogenic bacteria in real clinical samples. The results on bacteria agreed well with those obtained by conventional culture-based assays, as illustrated in Fig. 5.7d.

Vo-Dinh's group devised a label-free DNA biosensor based on molecular sentinel (MS) immobilized on a metal film over nanosphere (MFON) [71, 74–76]. Upon DNA hybridization, the Raman label at the end of the MS is separated from the MFON's surface to exhibit decreased Raman signal, which works as the readout and renders high selectivity in multiplexed analysis. With the initial detection of human RSAD2 gene [71] and Ki-67 DNA [74] and the multiplexed detection of IFI27 A and IFI44L [75], the group developed the biosensor into a bioassay-on-chip platform and detected ssDNA of dengue virus (LOD ~6 attomoles), which is the culprit of dengue fever that plagues 230–390 million people each year. The platform can be combined with microfluidics for on-chip sample preparation and detection, providing a new tool for POC diagnostics and global healthcare.

Detection of microRNAs (miRNAs) has been a key topic in cancer research, diagnosis, and prognosis. miRNAs can repress gene expression in a sequence-dependent manner [77] and are associated with various human diseases such as diabetes, Alzheimer's, and cancers [78–80]. At an early stage of cancer, extremely low concentrated miRNAs circulate in human body fluid, making detection of miRNAs with improved LOD and sensitivity desirable for early disease diagnosis and implementation of new treatment options [81].

Joshi et al. designed a regenerative LSPR-based miRNA sensor for early diagnosis of pancreatic ductal adenocarcinoma (PDAC), a deadly cancer with an overall 5-year survival rate of 7%. The cancer is hard to be detected when the tumor is small and at nonmetastatic stage [82, 83]. The sensor is based on gold nanoprisms functionalized with –S-C6-ssDNAs. Direct hybridization between the –S-C6-ssDNAs and the target miRNAs forms DNA duplex (Fig. 5.7e), which increases the refractive index in local environment of the nanoprism and redshifts the LSPR peak wavelength. The high sensitivity down to 10^{-18} M for specific miRNA-10b

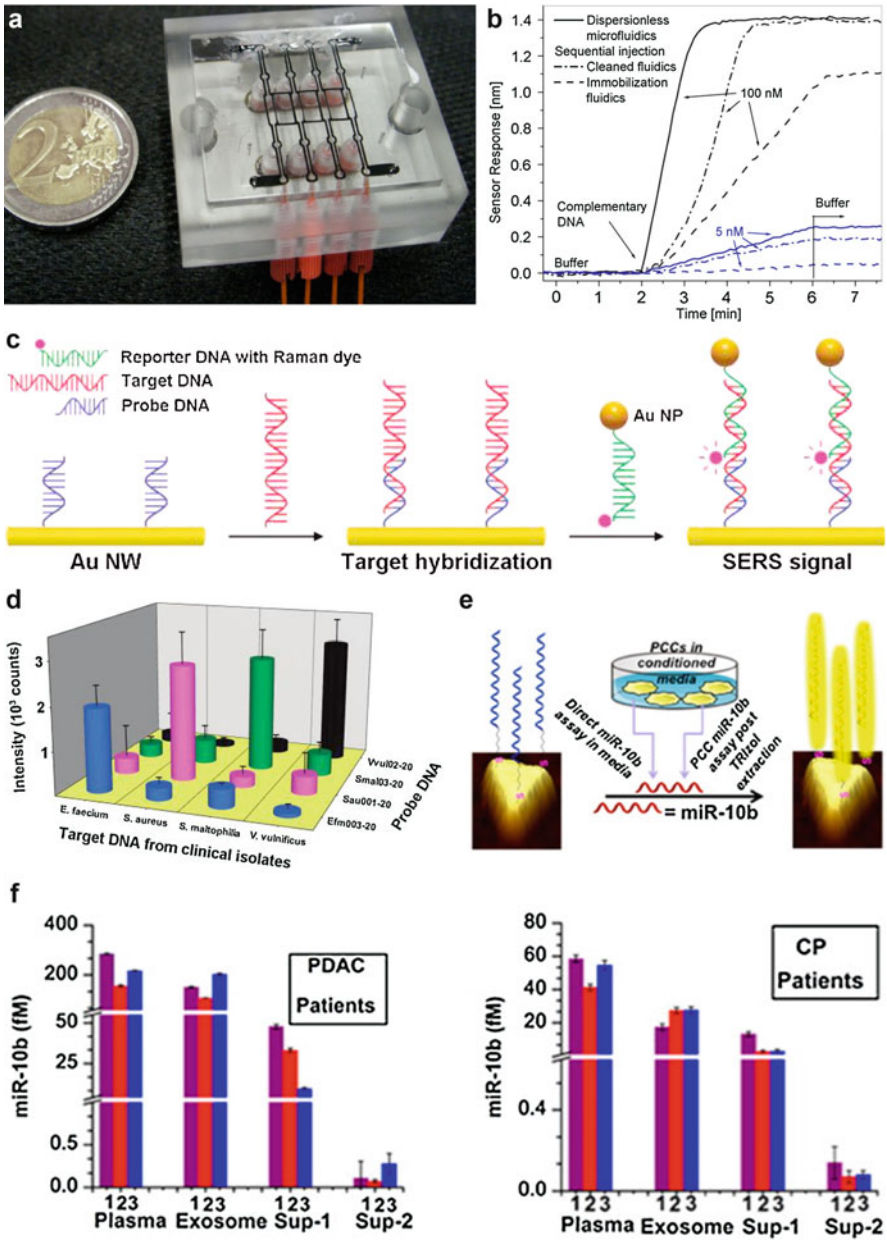

Fig. 5.7 (continued)

benefits from multiple factors: (a) atomically flat surface of the nanoprisms allowing efficient duplex formation, (b) high charge density of the duplex greatly altering the local refractive index, and (c) strong field enhancement at the tips of nanoprisms. Detection of miRNA-10b at a low concentration was achieved in pancreatic cancer cell lines, derived tissue culture media, human plasma, and plasma exosomes. Quantification of miRNA-10b in highly purified exosomes that were isolated from patients with PDAC and chronic pancreatitis (CP) was shown in Fig. 5.7f. PDAC patients had much higher miRNA-10b levels than CP patients. Integration of the sensor into microfluidics is expected to further enhance the miRNA measurements and the disease diagnosis with identifiable miRNA signatures.

5.2.2 Detection of Proteins

Proteins in biofluids such as serum are highly associated with biological functionalities. Detection of proteins and analysis of their unique sequences have high clinical relevance [84, 85]. For instance, a protein biomarker called SVEGFR-1 was increasingly expressed in patients with myelodysplastic syndromes (MDS), i.e., a diverse group of clonal disorders of the hematopoietic stem cell. Prostate-specific antigen (PSA) shows increased levels above the normal limits (4 ng mL^{-1}) in serum for possible prostate malignancy, which can be used for diagnosis and prognosis of prostate cancer [86]. Plasmofluidic immunoassays and immunosensors feature parallel, label-free, and real-time detection of proteins with high sensitivity, selectivity, multiplicity, and reproducibility [30, 87–90]. They are also applied to investigate protein-protein interaction [91], monitor live cell secretory events [92], and identify diagnosis-related cells [93].

SPP-based plasmofluidic sensors for label-free detection of proteins have recently been implemented on a smartphone platform [94]. A plasmonic sensor with dispersionless microfluidics was developed to detect protein biomarker of MDS disease (i.e., sVEGFR-1) via interaction with its high-affinity bio-receptor VEGF-A [95]. A detection limit of 25 ng/mL was achieved in 2% human blood plasma by using the sequential injection approach. However, the traditional experimental design that relies on a specific bio-receptor (known as "lock-and-key" approach) is limited by interference from molecules that are structurally or chemically alike. Moreover, most diseases are associated with multiple biomarkers, which necessitate

Fig. 5.7 Detection of DNAs and RNAs with plasmofluidic sensors. (**a**) Photograph of a four-channel flow cell for dispersionless microfluidics that was implemented in SPP-based detection of nucleic acid. (**b**) Comparison of sensor responses of different microfluidic designs in SPP-based detection of DNA E441C from *E. coli* cells (Reproduced with permission [31]. Copyright 2009 Elsevier Publishing). (**c**) Schematic illustration for the SERS-based detection of target DNAs by gold-particle-on-wire system. (d) Identification of target DNAs from clinical isolates with the gold-particle-on-wire sensor (Reproduced with permission [69]. Copyright 2010 American Chemical Society). (**e**) Schematic illustration of –S-C6-ssDNA-functionalized gold nanoprisms for LSPR-based sensing of miR-10b. (**f**) Determination of miR-10b concentration in plasma samples for three patients with PDAC and CP using the LSPR-based sensors (Reproduced with permission [83]. Copyright 2015 American Chemical Society)

the detection of a total protein distribution rather than a particular protein. To address these challenges, Choi et al. developed a "cross-reactive"-based sensor using a substrate of multiple segments of surfaces that are pre-adsorbed by different types of proteins. A distinctive pattern of SPP angle shifts arose from the interaction of the substrate with a sample of variable proteins [84]. The SPP angle pattern was used to clarify the concentration distributions of proteins and a specific biomarker, C-reactive protein (CRP), in a cocktail sample.

A more powerful way for simultaneous detection of multiple proteins is the use of protein microarrays in conjunction with surface plasmon resonance imaging (SPRI) [30]. However, protein microarrays often involve time-consuming fabrication process. Dehydrated or denatured proteins suffer a shorter lifetime of normal functionality. To overcome these problems, a multiplexed enzymatic synthesis via surface-coupled transcription-translation was employed for in vitro fabrication of protein microarrays and for their immediate use in biosensing based on a microfluidic platform, as illustrated in Fig. 5.8a–c. The plasmofluidic system includes generator, control, and detector components. Multiple RNA transcripts were created at the generator through surface reaction of RNA polymerase with adsorbed dsDNA and translated into proteins by cell-free protein synthesis. The synthesized proteins diffused to the detector element and formed protein microarrays. As a demonstration, binding of anti-GFP and antiluciferase to the protein arrays was characterized with SPRI and time-resolved absorption kinetic measurement, as shown in Fig. 5.8d–g. With multiple surface chemistries, the plasmofluidic system can be further implemented for multiplexed SPRI biosensing in clinical practices.

More challenges arise for SPP-based sensing in human serum samples due to (i) high nonspecific interaction between the sensor surface and serum proteins and (ii) matrix effects of serum such as high refractive index and viscosity that mask the binding events between the recognition elements on the sensor surface and the analytes in the serum [86]. Uludag et al. used a matrix elimination buffer to eliminate nonspecific binding of 98% serum proteins and performed a sandwich assay, in which the target proteins were sandwiched between a bottom layer of capture antibody and a top layer of antibody-modified Au NPs [86]. The Au NPs reduced the refractive-index mismatch between the buffer and the sample, leading to amplified SPP signal and enhanced sensitivity. A LOD of 0.29 ng mL^{-1} for tPSA in 75% human serum was attained, which was comparable to that achieved by a quartz crystal microbalance (QCM) sensor. SPP and QCM sensors were further combined to detect sub-attomolar human α-thrombin [96]. The sandwich immunoassays with SPP-based sensors are expected to improve early-stage cancer diagnosis and prognosis.

LSPR-based plasmofluidic sensors enable high-end miniaturization down to the single-nanoparticle scale [87, 97–100]. Zijlstra et al. reported real-time, label-free detection of single-protein binding events by monitoring the LSPR of a nanorod with an ultrasensitive photothermal assay [98]. When a single protein binds to the receptors on the surface of the nanorod, a small redshift of the longitudinal LSPR wavelength changes the absorption cross section of the nanorod at the wavelength of the heating beam, which can be measured with the transduced temperature change. Unlike the resonance Rayleigh scattering, the contrast scale of photothermal

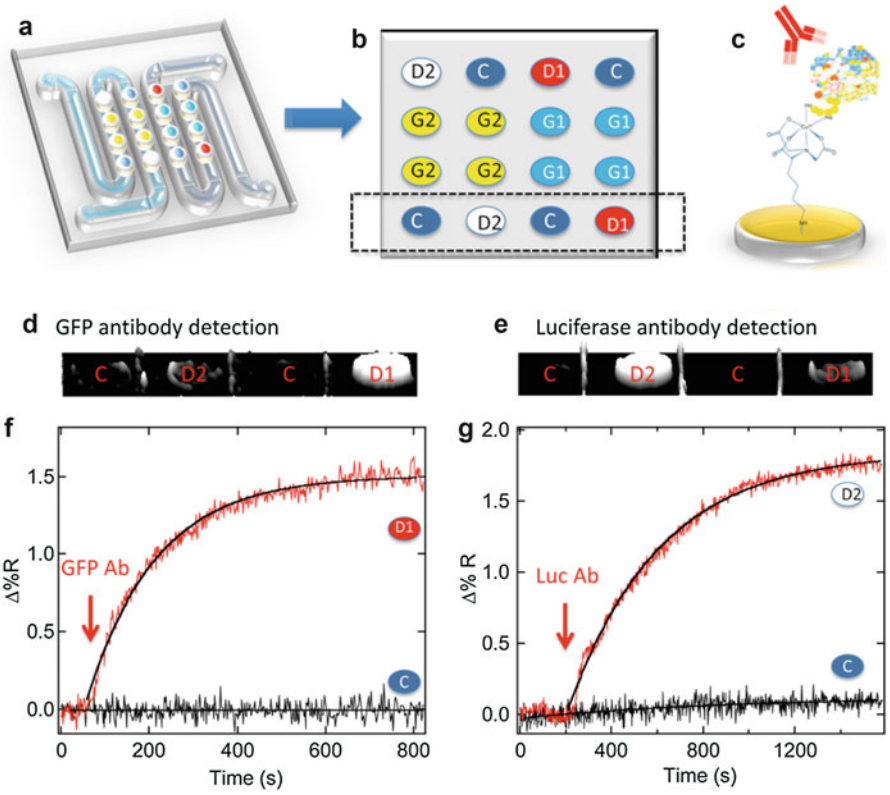

Fig. 5.8 Detection of proteins with SPP-based plasmofluidic sensors. (**a**) Schematic illustration and (**b**) spatial diagram of a GFP-luciferase DNA microarray in a dual-channel microfluidic cell. (**c**) Schematic illustration of antibody bound onto the synthesized protein array. SPRI difference images taken before and after the exposure to (**d**) anti-GFP and (**e**) antiluciferase solutions. Real-time SPRI adsorption kinetic measurement of (**f**) anti-GFP- and (**g**) antiluciferase-specific binding (Reproduced with permission [30]. Copyright 2012 American Chemical Society)

microscopy permits the measurement of mode volume that is commensurate to the size of a protein.

Ament et al. utilized single gold nanorods to monitor single-protein conformational dynamics and equilibrium coverage fluctuations [99]. The latter contain the information on the binding kinetics and nonequilibrium thermodynamics. By using a white light laser, an intensified CCD camera, and an engineered nanoparticle geometry, they achieved considerable improvement of signal-to-noise (SNR) ratio and time resolution over previous techniques to identify single-molecule binding events. Rather than utilizing passive surface binding to capture the proteins, Gordon's group used a double nanohole to actively trap single proteins and to measure the single-protein binding events [100].

LSPR biosensors based on nanoparticle ensembles and microfluidics are more suitable for clinical applications because the ensembles allow statistically significant

data analysis, relax constraints by nanoparticle variations, and enable simple instrumentation, fast data acquisition, and improved signal-to-noise ratio [87]. Plasmonic nanotechnologies such as plasmonic arrays [87, 88, 101–103] and SPRI [104, 105] and innovative microfluidic techniques such as integrated concentration gradient generator [104] and multi-well fluidic measurement [106] have been intensely pursued to detect and quantify cancer biomarkers with enhanced sensitivity, robustness, integrity, high throughput, and multiplexity.

Quidant's group developed a parallel and high-throughput LSPR-based plasmofluidic sensor that can be upgraded to a lab-on-a-chip system and be translated to clinical environments (Fig. 5.9a) [87]. For the sensor, a periodic array of gold nanorods with a bio-recognition layer was integrated with a microfluidic network. The authors applied the sensor to detect AFP and PSA, which are indicators of prostate cancers, at a LOD of as low as 5 ng/mL and a timescale of minutes. Chen et al. developed a highly integrated, multiarrayed LSPR sensor for massively parallel high-throughput detection of multiple cytokine biomarkers in a low-volume assay, as shown in Fig. 5.9b [88]. Consisting of 480 LSPR sensing spots with multistep processing for eight different samples, including manual loading, incubation, and washing, the sensor allowed quantitative measurements at concentrations ranging from 10 to 10,000 pg/mL in a 1-μL sample of serum. It also enabled multianalyte detection of ten cycles for each sample in 40 min, which is more than ten times shorter than traditional sandwich immunoassays. The sensor was further applied to measure cytokine levels of IL-6 and IL-10 in two neonates, who received cardiopulmonary bypass surgery for congenital heart disease within 24 h. The measurement was valuable for defining the postsurgery responses and predicting the anticipated assay outcomes.

Measuring binding affinities between proteins is also of fundamental interest and clinical significance. A "nanoSPR" method was proposed to simultaneously characterize the binding affinities among many macromolecular partners [91]. Briefly, multiple batches of gold nanorods functionalized with different proteins and one batch without functionalization (as a reference) were driven through the flow cell consecutively to generate a positon-encoded sensor. The encoding of the sensor was carried out by repetitive recording of the position of each randomly deposited gold nanorod, as shown in Fig. 5.9c. As a demonstration, the sensor was applied to study the interactions of three bacterial division proteins with a target protein FtsZ, which is an essential element of the division machinery in most bacterial systems. The results had an excellent agreement with those by conventional composition gradient static light scattering and fluorescence anisotropy. With the small device size, reduced sample volume, and built-in statistics, the sensor is envisioned to be a powerful tool in drug screening and discovery applications.

In light of the important role of cell secretion in a variety of physiological processes, Wu et al. developed a label-free, ultrasensitive, plasmofluidic platform based on gold nanoslits with strong Fano resonance to monitor dynamic live cell secretory activities [92]. The THP1 cells were trapped and cultured in microfluidic channels with the sensing surface of gold nanoslits ~3–5 μm away from the cell membrane. Upon stimulation with continuous lipopolysaccharide, the cells were

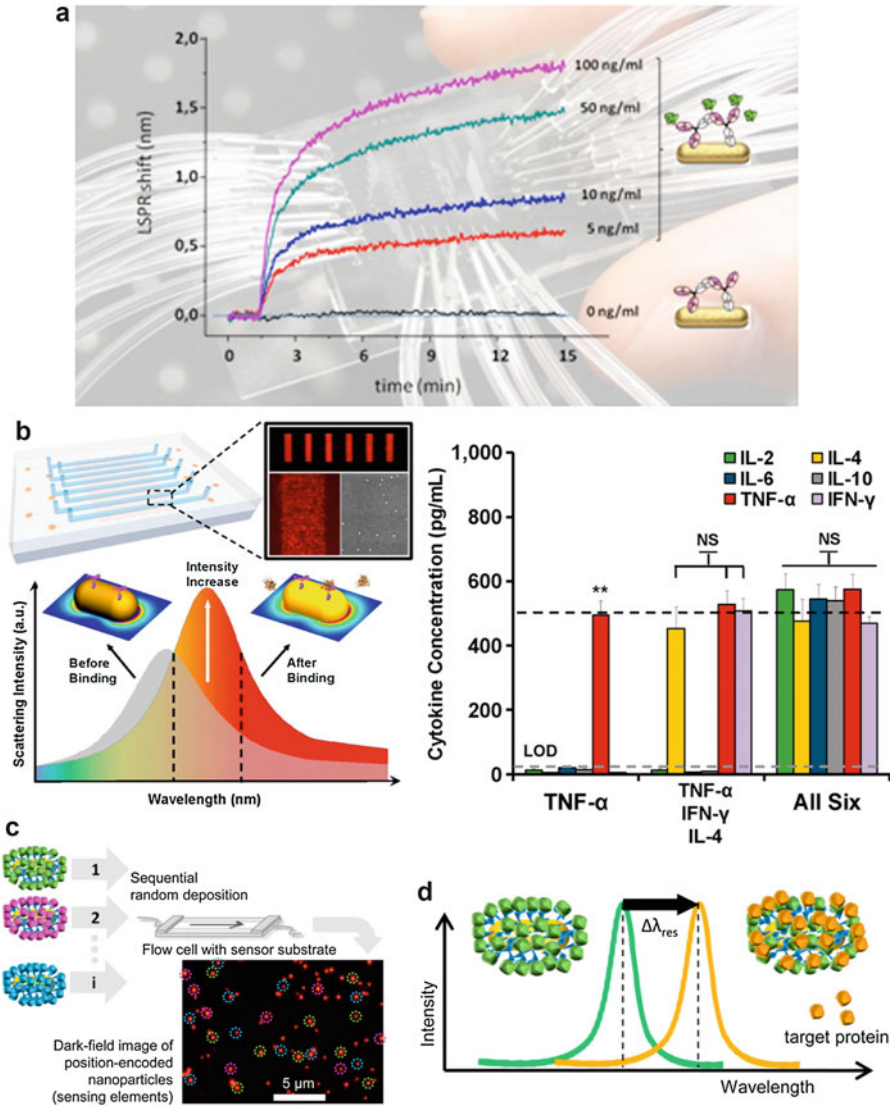

Fig. 5.9 Detection of proteins with LSPR-based plasmofluidic sensors. (**a**) Detection of prostate cancer biomarkers down to a concentration of 5 ng/mL in a complex matrix (consisting of 50% human serum) with a microfluidics-integrated LSPR-based biosensor (Reproduced with permission [87]. Copyright 2014 American Chemical Society). (**b**) Multiplex immunoassays of six cytokines in a complex serum matrix with a high-throughput, label-free, multiarrayed LSPR biosensor chip (Reproduced with permission [88]. Copyright 2015 American Chemical Society). (**c**) Simultaneous characterization of binding affinities between multiple protein partners with a LSPR biosensor. (**d**) Working principle of the characterization of binding affinities (Reproduced with permission [91]. Copyright 2014 American Chemical Society)

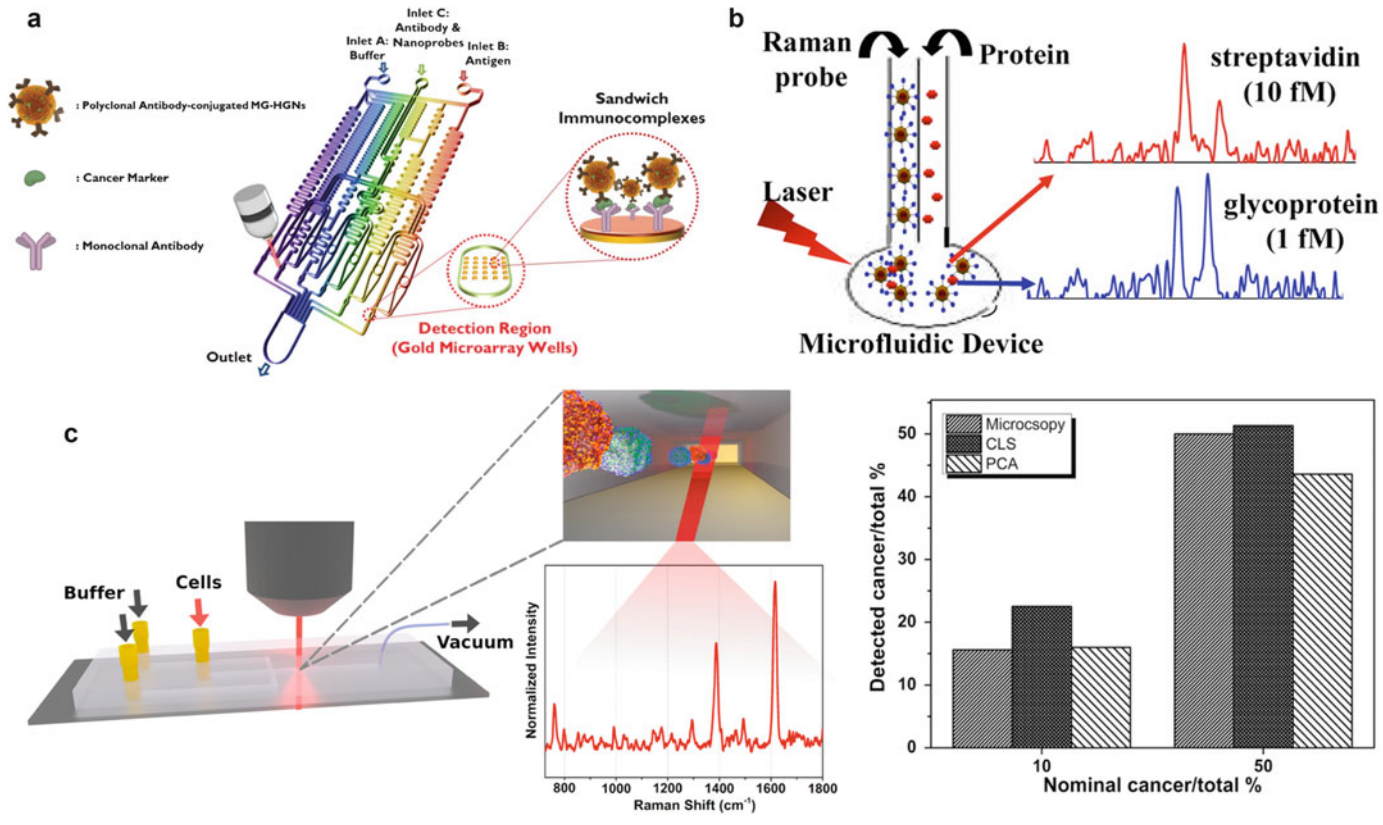

Fig. 5.10 Detection of proteins with SERS-based plasmofluidic sensors. (**a**) Schematic representation of a SERS-based immunoassay consisted of a structured gold array integrated with gradient microfluidics. The illustrations in the enlarged circles represent the formation of sandwich immunocomplexes on the surface

found to secrete MMP-9 proteins in 2 h. The plasmofluidic sensor needs less than ten cells for the study, while ELISA analysis demands at least a few thousand cells. The sensor can be applied for fundamental study of secretory events in different physiological environments and medical diagnosis of various diseases at the single-cell level.

SERS-based immunoassay is considered another promising approach for protein sensing. One of the most popular strategies uses a sandwich immunocomplex protocol with antibody-conjugated metal particles [89, 108–111]. Choo's group implemented magnetic tweezers [108] and optoelectronic tweezers [109] in a gradient microfluidic channel to form sandwich immunocomplexes for the sensitive and automatic quantitative analysis in less than 30 min. In the immunocomplexes, target antigens were sandwiched between antibody-conjugated microspheres and antibody-conjugated SERS-active nanoparticles. The magnetic tweezer-based immunoassay had a LOD of 1–10 ng/mL for rabbit IgG, and the optoelectronic tweezer-based one achieved a LOD of 98 pg/mL for alpha-fetoprotein (AFP). The same group further integrated sandwich immunoassay [110] with gradient microfluidics to achieve programmable and automatic analysis of biomarkers with small sample volume, easy sample preparation, and short assay time [89]. After the AFP antigens were captured by the immobilized antibodies on gold microwells, polyclonal anti-AFP antibody-conjugated particles were attached to form the sandwich immunocomplexes, as shown in Fig. 5.10a. A similar methodology was applied to detect hepatitis B virus antigen in human blood and blood plasma. Hepatitis B virus infection is a common cause of chronic liver disease worldwide [112]. Using a sandwich-typed immunoassay, Zou et al. detected carcinoembryonic antigen in raw blood samples with a LOD of as low as 10^{-12} M. Carcinoembryonic antigen is a wide-spectrum biomarker for diagnosis of various cancers [111].

Formation of stable electromagnetic "hot spots" in nanoparticle aggregates is another strategy for SERS-based protein analysis with high reproducibility and sensitivity. Saha et al. designed a paper-based microfluidic SERS system to detect streptavidin and glycoprotein with pico to femtomolar concentration, as shown in Fig. 5.10b [107]. Two channels with Ag/Au nanoparticles and proteins merge into a small round-shaped reaction chamber to generate SERS-active nanoparticle aggregates via protein-assisted cross-linking. Notably, the porous feature of the microchannels regulates the extent of nanoparticle aggregation and prevents the screening of "hot spots" in large aggregates.

Fig. 5.10 (continued) of a 5 × 5 array of round gold wells (Reproduced with permission [89]. Copyright 2013 RSC Publishing). (**b**) A paper-based microfluidic device for SERS-based protein detection. It involves the aggregation of Ag/Au nanoparticles at the presence of proteins (Reproduced with permission [107]. Copyright 2014 American Chemical Society). (**c**) Schematic representation of a SBT-based microfluidic system to distinguish cancer cells in a low concentration against background of normal cells. The bar graph compares cancer cell counts by microscopy, PCA, and CLS. The latter two are deconvolution strategies for analyzing the cancer-normal cell ratios with the composite Raman spectrum (Reproduced with permission [93]. Copyright 2015 American Chemical Society)

SERS protein biotags (SBTs) have been developed for identification of cells and pathogens in body fluids, which is significant for early disease detection and monitoring of patient response to therapy [93]. In the microfluidic cell identification system, two spectroscopically distinguishable SBTs that target distinct cell epitopes were used to label cells in a single focused line by hydrodynamic flow, as illustrated in Fig. 5.10c [93]. The identification was accomplished by measuring the relative signal from the cancer-specific SBT versus the cell-identifying universal control SBT. The discrimination efficiency can reach 1 cancer cell from a population of 100 normal cells due to spectroscopic richness of the Raman bands of the reporter molecules on the two SBTs and algorithmic effectiveness of the two deconvolution strategies for the composite spectrum. The SBT approach provides a continuous, low-cost, and nondestructive tumor cell identification and paves the way toward clinical cancer diagnosis at the single-cell level.

5.2.3 Detection of Pathogens

The detection of infectious agents such as viruses and bacteria is critical for public health, homeland security, and food industry [113, 115, 117]. Viruses have been responsible for a number of epidemic outbreaks (e.g., H1N1 flu and SARS) in recent years. Timely virus detection becomes essential for recognizing and controlling future epidemics. Conventional techniques such as cell culture methods, PCR, and ELISA can detect and quantify pathogens with high sensitivity and specificity [118, 119]. However, they require lab-intensive procedures, expensive equipment, and well-trained operators. Alternative biosensing techniques that can achieve reliable, accurate, and sensitive detection and analysis of pathogens under the variable settings, including source-limited settings and primary care settings, are in great need. Among the various detection platforms that use different mechanisms such as electrical, mechanical, and optical signal transduction [2, 5, 120], plasmofluidic biosensors are promising for label-free detection of infectious agents.

Wang et al. achieved label-free imaging, detection, and mass/size measurement of single viral particles with high-resolution surface plasmon resonance spectroscopy [121]. The viral particles were imaged as diffraction patterns from their scattering of SPP. The particle size and mass were determined from the image intensities. Two viruses, i.e., H1N1 influenza A/PR/8/34 and HCMV, were studied with a mass detection limit of 1 ag, which is four orders of magnitude lower than that by conventional surface plasmon resonance method.

To meet the needs for quickly recognizing and controlling epidemics, a plasmofluidic sensor was developed to detect viruses from biologically relevant media, as illustrated in Fig. 5.11a [113]. The sensor exploits plasmon-enhanced extraordinary light transmission through metal nanohole arrays and is applicable to a broad range of pathogens. It was applied to detect PT-Ebola virus in PBS buffer solution based on the consistent redshift (>14 nm) of the plasmon resonance wavelength. A 4-nm shift in resonance wavelength was observed for virus detection in biological media consisted of cell growth medium and 7% fetal calf serum. The detectable virus concentration ranges from 10^6 to 10^9 PFU/mL, which is relevant to both clinical testing and drug screening.

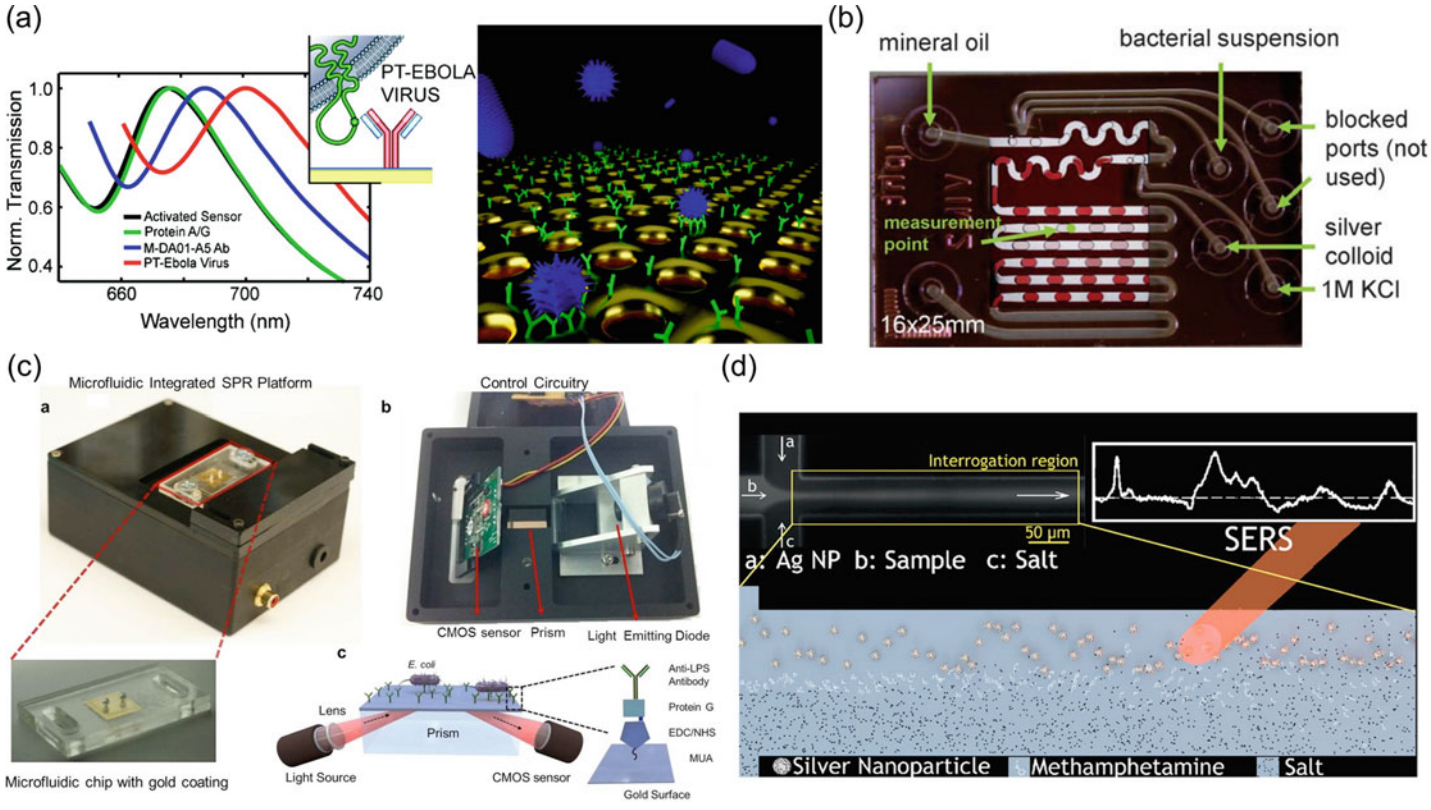

Fig. 5.11 Detection of pathogens and drugs with plasmofluidic sensors. (**a**) Detection of PT-Ebola virus using a plasmofluidic biosensor based on extraordinary optical transmission in metal nanohole arrays functionalized with M-DA01-A5 antibodies (Reproduced with permission [113]. Copyright 2010 American

Inci et al. developed a plasmofluidic platform for label-free, high-sensitive, high-specific, and reproducible HIV viral load quantification from unprocessed whole blood sample [117]. Surface chemistry and highly specific antibody immobilization were applied to capture the viruses at the electromagnetic "hot spots" and to minimize background signal from nonspecific binding of blood cells. Briefly, poly-L-lysine-modified polystyrene with terminal amine group was used as substrates to capture gold nanoparticles. The gold nanoparticles were treated with different chemicals consecutively, including 11-mercaptoundecanoic acid, *N*-ethyl-*N*-(3-dimethylaminopropyl)carbodiimide hydrochloride, N-hydroxysulfosuccinimide, NeutrAvidin, and biotinylated anti-gp120 polyclonal antibody. The antibody was positioned in a favorable orientation to have a high capture efficiency for the viruses. A SPP platform based on DNA-RNA hybridization was also developed to detect viruses plaguing plant food and feed crop plants [122].

Rapid detection of bacteria makes a difference in monitoring and preventing outbreaks of infections [2, 118]. For this purpose, Walter et al. developed microfluidic SERS to discriminate bacteria based on strain levels in a fast and reliable fashion [114]. In their plasmofluidic system, aqueous analytes and colloid solution form droplets in mineral oil, creating a segmented flow for stable optical measurements and reproducible bacterial identification, as shown in Fig. 5.11b. Besides colloidal nanoparticles, solid-state SERS substrate functionalized with recognition molecules was also employed to capture and analyze *E. coli* cells with high specificity and sensitivity [123].

Demirci's group developed a portable microfluidic SPP platform that can rapidly detect and quantify *E. coli* and *S. aureus* [115]. All the elements, including light source, optical components, CMOS sensor, circuitry, and microfluidic chip, were packaged in a portable box with dimensions of 13.5 cm × 10 cm × 5.2 cm, as shown in Fig. 5.11c. Effective capture and detection of *E. coli* at concentrations from ~10^5 to 3.2 × 10^7 CFUs/mL in PBS and peritoneal dialysis fluid were demonstrated. Multiplicity and specificity were tested with *S. aureus* in PBS solution, implying the potential of the platform for pathogen diagnostics at both POC and primary care settings.

5.2.4 Detection of Drugs

Quick and cost-effective pharmaceutical analysis can benefit healthcare, biomedicine, and food safety [124]. For example, drug screening is a critical step in new drug discovery. Detection of drug residues in food and human liquids is frequently needed

Fig. 5.11 (continued) Chemical Society). (**b**) Discrimination of bacteria based on strain levels using a six-port SERS-based plasmofluidic biosensor. Mineral oil was used as separation medium to prevent deposition of nanoparticles and analytes on the substrate (Reproduced with permission [114]. Copyright 2011 RSC Publishing). (**c**) Detection and quantification of *E. coli* cells with a portable SPP-based plasmofluidic sensor (Reproduced with permission [115]. Copyright 2015 Nature Publishing Group). (**d**) Detection of trace concentrations of drugs in saliva with a SERS-based plasmofluidic sensor. No chemical functionalization and reactants were required for the detection (Reproduced with permission [116]. Copyright 2013 American Chemical Society)

for food safety and healthcare. The capability of monitoring antibody-polypeptide reaction is desirable for multiplexed drug discovery. Chen et al. proposed a SPRI-based visualization method for monitoring antibody-polypeptide binding in a label-free and high-throughput format [125]. The plasmonic platform can support the dynamic imaging of polypeptide microarray and the time tracing of 3D histograms for monitoring antibody-polypeptide reaction on the surface.

Chiral compounds have significant impacts on pharmacological and biological processes. Effective strategies for chiral discrimination and enantioseparation are highly needed to meet the increasing need for enantiomerically pure compounds. For a pair of enantiomers, it is possible that one configuration is active drug, while the other configuration remains inactive, contributes to side effects, displays toxicity, or works as an antagonist [126, 127]. As an example, Guo et al. demonstrated α-thrombin-functionalized LSPR sensor integrated with a microfluidic chip for enantioselective analysis of melagatran. Recently, we have achieved high-sensitive label-free chiral sensing for drug molecules based on moiré chiral metamaterials [128].

Plasmofluidic sensors were also developed for label-free and rapid detection of drug residues in food and clinical samples [129]. Fernandez et al. used a portable six-channel SPP sensor to analyze antibiotic residues from different families, i.e., fluoroquinolones, sulfonamides, and phenicols, in whole milk samples [130]. The sensor showed good regenerative ability and repeatability and accomplished LODs far below the maximum residue levels established by the European Union for the antibiotics. Zhao et al. used a multichannel SPP sensor to analyze the concentrations of methotrexate, an anticancer drug, in the serum of a patient undergoing chemotherapy treatments. The results agreed with those by fluorescence polarization immunoassay [131].

Andreou et al. developed a microfluidic SERS to identify drugs at clinical levels without specialized chemicals and bio-reagents [116]. As shown in Fig. 5.11d, a laminar flow consisted of a central stream of analytes (i.e., methamphetamine) and two sheath streams of silver nanoparticle and salt solutions was created. At the interrogation region, SERS-active nanoparticle dimers and small-order aggregates with methamphetamine predominantly formed. Due to the low affinity of methamphetamine to the silver nanoparticles, the salt was added to induce the aggregation. Trace concentrations of methamphetamine in saliva were detected within minutes. The microfluidic SERS will find applications in detecting many other health-related molecules such as toxins and pollutants.

6 Conclusions and Future Perspectives

Tremendous progress has been made in plasmofluidics for biological analysis and medical diagnostics. In particular, plasmonic tweezers achieved noninvasive trapping of biological cells, DNAs, and proteins at the single-entity level. 3D manipulations were demonstrated with plasmonic tweezers based on an optical fiber tip with high-resolution mechanical motion control. Long-range and rapid delivery of nanoparticles was achieved with electrothermoplasmonics. Most of the current tweezers used microfluidic channels as passive containers for sample solutions. It is

anticipated that future plasmonic tweezers will fully reap the benefits of micro-/nanofluidics to further enhance their functionalities for biosensing and diagnostic applications. In particular, the light-fluid interactions at the nanoscale can be explored to achieve versatile multifunctional plasmofluidic tweezers [7]. Our preliminary study indicated that the plasmon-enhanced photothermal effects such as thermophoresis are one of the promising strategies for optical manipulations in variable fluidic environments.

A variety of plasmofluidic sensors has been developed to detect and analyze nucleic acids, proteins, pathogens, and drugs in life sciences, disease diagnostics, and drug discovery. Innovative microfluidic design, plasmonic engineering, and surface functionalization have led to sensitive, robust, and label-free POC biosensors. The next-generation plasmofluidic sensors are expected to target at translational and clinical applications [4]. For the purpose, the sensors need to be a highly integrated, robust, and user-friendly system that can handle a variety of clinical samples such as urine, blood, and saliva and enables POC diagnostics at field settings.

In summary, the highly interdisciplinary field of plasmofluidics presents exciting opportunities for new discoveries and POC devices. With the stronger collaborations among researchers from physics, chemistry, biology, pharmacology, and engineering, as well as clinicians and entrepreneurs, plasmofluidics for biosensing and disease diagnostics will continue to grow and contribute to global healthcare.

Acknowledgments The authors acknowledge the financial support of the Beckman Young Investigator Program and the Office of Naval Research Young Investigator Program.

References

1. Tokel O, Inci F, Demirci U (2014) Advances in plasmonic technologies for point of care applications. Chem Rev 114(11):5728–5752
2. Zhang W et al (2016) Portable point-of-care diagnostic devices. Anal Methods 8 (44):7847–7867
3. Siegel RL, Miller KD, Jemal A (2016) Cancer statistics, 2016. CA Cancer J Clin 66(1):7–30
4. Sin MLY et al (2014) Advances and challenges in biosensor-based diagnosis of infectious diseases. Expert Rev Mol Diagn 14(2):225–244
5. Pai NP et al (2012) Point-of-care testing for infectious diseases: diversity, complexity, and barriers in low- and middle-income countries. PLoS Med 9(9):e1001306
6. Han KN, Li CA, Seong GH (2013) Microfluidic chips for immunoassays. In: Cooks RG, Pemberton JE (eds) Annual review of analytical chemistry, vol 6. Annual Reviews, Palo Alto, pp 119–141
7. Wang M et al (2015) Plasmofluidics: merging light and fluids at the micro-/nanoscale. Small 11(35):4423–4444
8. Barnes WL, Dereux A, Ebbesen TW (2003) Surface plasmon subwavelength optics. Nature 424(6950):824–830
9. Zheng YB et al (2012) Molecular plasmonics for biology and nanomedicine. Nanomedicine 7(5):751–770
10. Juan ML, Righini M, Quidant R (2011) Plasmon nano-optical tweezers. Nat Photonics 5(6):349–356

11. Wang DS, Fan SK (2016) Microfluidic surface plasmon resonance sensors: from principles to point-of-care applications. Sensors 16(8):1175
12. Mayer KM, Hafner JH (2011) Localized surface plasmon resonance sensors. Chem Rev 111(6):3828–3857
13. Singh P (2016) SPR biosensors: historical perspectives and current challenges. Sensors Actuators B Chem 229:110–130
14. Huang JS, Yang YT (2015) Origin and future of plasmonic optical tweezers. Nano 5(2):1048–1065
15. Zheng YB et al (2008) Systematic investigation of localized surface plasmon resonance of long-range ordered Au nanodisk arrays. J Appl Phys 103(1):014308
16. Garcés-Chávez V, Dholakia K, Spalding GC (2005) Extended-area optically induced organization of microparticles on a surface. Appl Phys Lett 86(3):031106
17. Wang K et al (2010) Scannable plasmonic trapping using a gold stripe. Nano Lett 10(9):3506–3511
18. Wang XD et al (2013) Theoretical and experimental study of surface plasmon radiation force on micrometer-sized spheres. Plasmonics 8(2):637–643
19. Righini M et al (2007) Parallel and selective trapping in a patterned plasmonic landscape. Nat Phys 3(7):477–480
20. Grigorenko AN et al (2008) Nanometric optical tweezers based on nanostructured substrates. Nat Photonics 2(6):365–370
21. Kang J-H et al (2011) Low-power nano-optical vortex trapping via plasmonic diabolo nanoantennas. Nat Commun 2:582
22. Roxworthy BJ et al (2012) Application of plasmonic bowtie nanoantenna arrays for optical trapping, stacking, and sorting. Nano Lett 12(2):796–801
23. Zheng Y et al (2014) Nano-optical conveyor belt, part II: demonstration of handoff between near-field optical traps. Nano Lett 14(6):2971–2976
24. Lin L et al (2016) Bubble-pen lithography. Nano Lett 16(1):701–708
25. Juan ML et al (2009) Self-induced back-action optical trapping of dielectric nanoparticles. Nat Phys 5(12):915–919
26. Baffou G, Quidant R, García de Abajo FJ (2010) Nanoscale control of optical heating in complex plasmonic systems. ACS Nano 4(2):709–716
27. Baffou G et al (2013) Photoinduced heating of nanoparticle arrays. ACS Nano 7(8):6478–6488
28. Donner JS et al (2011) Plasmon-assisted optofluidics. ACS Nano 5(7):5457–5462
29. Puiu M, Bala C (2016) SPR and SPR imaging: recent trends in developing nanodevices for detection and real-time monitoring of biomolecular events. Sensors 16(6):870
30. Seefeld TH, Halpern AR, Corn RM (2012) On-chip synthesis of protein microarrays from DNA microarrays via coupled in vitro transcription and translation for surface plasmon resonance imaging biosensor applications. J Am Chem Soc 134(30):12358–12361
31. Springer T, Piliarik M, Homola J (2010) Surface plasmon resonance sensor with dispersionless microfluidics for direct detection of nucleic acids at the low femtomole level. Sensors Actuators B-Chem 145(1):588–591
32. Lee Y et al (2013) Tunable directive radiation of surface-plasmon diffraction gratings. Opt Express 21(3):2748–2756
33. Krupin O et al (2013) Biosensing using straight long-range surface plasmon waveguides. Opt Express 21(1):698–709
34. Szunerits S, Boukherroub R (2012) Sensing using localised surface plasmon resonance sensors. Chem Commun 48(72):8999–9010
35. Unser S et al (2015) Localized surface plasmon resonance biosensing: current challenges and approaches. Sensors 15(7):15684–15716
36. Escobedo C et al (2010) Flow-through vs flow-over: analysis of transport and binding in nanohole array plasmonic biosensors. Anal Chem 82(24):10015–10020
37. Escobedo C et al (2012) Optofluidic concentration: plasmonic nanostructure as concentrator and sensor. Nano Lett 12(3):1592–1596

38. Lee SY et al (2011) High-fidelity optofluidic on-chip sensors using well-defined gold nanowell crystals. Anal Chem 83(23):9174–9180
39. Verellen N et al (2011) Plasmon line shaping using nanocrosses for high sensitivity localized surface plasmon resonance sensing. Nano Lett 11(2):391–397
40. Zhang SP et al (2011) Substrate-induced Fano resonances of a plasmonic nanocube: a route to increased-sensitivity localized surface plasmon resonance sensors revealed. Nano Lett 11(4):1657–1663
41. Shen Y et al (2012) Tuning the plasmon resonance of a nano-mouth array. Nanoscale 4(18):5576–5580
42. Shen Y et al (2013) Plasmonic gold mushroom arrays with refractive index sensing figures of merit approaching the theoretical limit. Nat Commun 4:2381
43. Lin L, Zheng Y (2015) Engineering of parallel plasmonic–photonic interactions for on-chip refractive index sensors. Nanoscale 7(28):12205–12214
44. Lin L, Zheng Y (2015) Optimizing plasmonic nanoantennas via coordinated multiple coupling. Sci Rep 5:14788
45. Petryayeva E, Krull UJ (2011) Localized surface plasmon resonance: nanostructures, bioassays and biosensing-a review. Anal Chim Acta 706(1):8–24
46. Chen K et al (2015) Moiré nanosphere lithography. ACS Nano 9(6):6031–6040
47. Wu Z et al (2015) Tunable multiband metasurfaces by moire nanosphere lithography. Nanoscale 7(48):20391–20396
48. Escobedo C (2013) On-chip nanohole array based sensing: a review. Lab Chip 13(13):2445–2463
49. Im H et al (2014) Label-free detection and molecular profiling of exosomes with a nanoplasmonic sensor. Nat Biotechnol 32(5):490–495
50. Willets KA, Duyne RPV (2007) Localized surface plasmon resonance spectroscopy and sensing. Annu Rev Phys Chem 58(1):267–297
51. Wong CL, Olivo M (2014) Surface plasmon resonance imaging sensors: a review. Plasmonics 9(4):809–824
52. White IM, Yazdi SH, Yu WW (2012) Optofluidic SERS: synergizing photonics and microfluidics for chemical and biological analysis. Microfluid Nanofluid 13(2):205–216
53. Cialla D et al (2012) Surface-enhanced Raman spectroscopy (SERS): progress and trends. Anal Bioanal Chem 403(1):27–54
54. Schlucker S (2014) Surface-enhanced Raman spectroscopy: concepts and chemical applications. Angew Chem-Int Ed 53(19):4756–4795
55. Huang JA et al (2015) SERS-enabled lab-on-a-chip systems. Adv Opt Mater 3(5):618–633
56. Zhou J et al (2012) Convenient formation of nanoparticle aggregates on microfluidic chips for highly sensitive SERS detection of biomolecules. Anal Bioanal Chem 402(4):1601–1609
57. Lin L et al (2016) Light-directed reversible assembly of plasmonic nanoparticles using plasmon-enhanced thermophoresis. ACS Nano 10(10):9659–9668
58. Righini M et al (2009) Nano-optical trapping of rayleigh particles and *Escherichia coli* bacteria with resonant optical antennas. Nano Lett 9(10):3387–3391
59. Huang L, Maerkl SJ, Martin OJF (2009) Integration of plasmonic trapping in a microfluidic environment. Opt Express 17(8):6018–6024
60. Shoji T et al (2013) Permanent fixing or reversible trapping and release of DNA micropatterns on a gold nanostructure using continuous-wave or femtosecond-pulsed near-infrared laser light. J Am Chem Soc 135(17):6643–6648
61. Nicoli F et al (2014) DNA translocations through solid-state plasmonic nanopores. Nano Lett 14(12):6917–6925
62. Pang Y, Gordon R (2011) Optical trapping of a single protein. Nano Lett 12(1):402–406
63. Zehtabi-Oskuie A et al (2013) Double nanohole optical trapping: dynamics and protein-antibody co-trapping. Lab Chip 13(13):2563–2568
64. Al Balushi, A.A. And R. Gordon A label-free untethered approach to single-molecule protein binding kinetics. Nano Lett, 2014. 14(10): p. 5787–5791

65. Ndukaife JC et al (2015) Long-range and rapid transport of individual nano-objects by a hybrid electrothermoplasmonic nanotweezer. Nat Nanotechnol 11:53. Advance online publication
66. Berthelot J et al (2014) Three-dimensional manipulation with scanning near-field optical nanotweezers. Nat Nanotechnol 9(4):295–299
67. Ndukaife JC, Shalaev VM, Boltasseva A (2016) Plasmonics-turning loss into gain. Science 351(6271):334–335
68. Lin L et al (2017) Thermophoretic tweezers for low-power and versatile manipulation of biological cells. ACS Nano 11:3147
69. Kang T et al (2010) Patterned multiplex pathogen DNA detection by Au particle-on-wire SERS sensor. Nano Lett 10(4):1189–1193
70. Huang C et al (2012) Gold nanoring as a sensitive plasmonic biosensor for on-chip DNA detection. Appl Phys Lett 100(17):173114
71. Ngo HT et al (2013) Label-free DNA biosensor based on SERS molecular sentinel on nanowave chip. Anal Chem 85(13):6378–6383
72. Wang H-N, Fales AM, Vo-Dinh T (2015) Plasmonics-based SERS nanobiosensor for homogeneous nucleic acid detection. Nanomedicine 11(4):811–814
73. Homola J (2008) Surface plasmon resonance sensors for detection of chemical and biological species. Chem Rev 108(2):462–493
74. Wang H-N et al (2013) Molecular sentinel-on-chip for SERS-based biosensing. Phys Chem Chem Phys 15(16):6008–6015
75. Ngo HT et al (2014) Multiplex detection of disease biomarkers using SERS molecular sentinel-on-chip. Anal Bioanal Chem 406(14):3335–3344
76. Ngo HT et al (2014) DNA bioassay-on-chip using SERS detection for dengue diagnosis. Analyst 139(22):5656–5660
77. Mukherji S et al (2011) MicroRNAs can generate thresholds in target gene expression. Nat Genet 43(9):854–859
78. Lu J et al (2005) MicroRNA expression profiles classify human cancers. Nature 435 (7043):834–838
79. Volinia S et al (2006) A microRNA expression signature of human solid tumors defines cancer gene targets. Proc Natl Acad Sci U S A 103(7):2257–2261
80. Jeffrey SS (2008) Cancer biomarker profiling with microRNAs. Nat Biotechnol 26(4):400–401
81. Arata H, Hosokawa K, Maeda M (2014) Rapid sub-attomole microRNA detection on a portable microfluidic chip. Anal Sci 30(1):129–135
82. Joshi GK et al (2014) Highly specific plasmonic biosensors for ultrasensitive microRNA detection in plasma from pancreatic cancer patients. Nano Lett 14(12):6955–6963
83. Joshi GK et al (2015) Label-free nanoplasmonic-based short noncoding RNA sensing at attomolar concentrations allows for quantitative and highly specific assay of microRNA-10b in biological fluids and circulating exosomes. ACS Nano 9(11):11075–11089
84. Choi S et al (2011) Monitoring protein distributions based on patterns generated by protein adsorption behavior in a microfluidic channel. Lab Chip 11(21):3681–3688
85. Masson J-F, Zhao SS (2015) Plasmonic sensors for analysis of proteins and an oncologic drug in human serum. In: Vestergaard MDC et al (eds) Nanobiosensors and nanobioanalyses. Springer Japan, Tokyo, pp 305–333
86. Uludag Y, Tothill IE (2012) Cancer biomarker detection in serum samples using surface plasmon resonance and quartz crystal microbalance sensors with nanoparticle signal amplification. Anal Chem 84(14):5898–5904
87. Acimovic SS et al (2014) LSPR chip for parallel, rapid, and sensitive detection of cancer markers in serum. Nano Lett 14(5):2636–2641
88. Chen P et al (2015) Multiplex serum cytokine immunoassay using nanoplasmonic biosensor microarrays. ACS Nano 9(4):4173–4181
89. Lee M et al (2012) SERS-based immunoassay using a gold array-embedded gradient microfluidic chip. Lab Chip 12(19):3720–3727

90. He J et al (2015) Patterned plasmonic nanoparticle arrays for microfluidic and multiplexed biological assays. Anal Chem 87(22):11407–11414
91. Ahijado-Guzmán R et al (2014) Plasmonic nanosensors for simultaneous quantification of multiple protein–protein binding affinities. Nano Lett 14(10):5528–5532
92. Wu SH et al (2013) Optofluidic platform for real-time monitoring of live cell secretory activities using Fano resonance in gold nanoslits. Small 9(20):3532–3540
93. Pallaoro A et al (2015) Rapid identification by surface-enhanced Raman spectroscopy of cancer cells at low concentrations flowing in a microfluidic channel. ACS Nano 9(4):4328–4336
94. Liu Y et al (2015) Surface plasmon resonance biosensor based on smart phone platforms. Sci Rep 5:12864
95. Pimkova K et al (2012) Surface plasmon resonance biosensor for the detection of VEGFR-1-a protein marker of myelodysplastic syndromes. Anal Bioanal Chem 402(1):381–387
96. He P et al (2014) Ultrasensitive detection of thrombin using surface plasmon resonance and quartz crystal microbalance sensors by aptamer-based rolling circle amplification and nanoparticle signal enhancement. Chem Commun 50(12):1481–1484
97. Truong PL, Kim BW, Sim SJ (2012) Rational aspect ratio and suitable antibody coverage of gold nanorod for ultra-sensitive detection of a cancer biomarker. Lab Chip 12(6):1102–1109
98. Zijlstra P, Paulo PMR, Orrit M (2012) Optical detection of single non-absorbing molecules using the surface plasmon resonance of a gold nanorod. Nat Nanotechnol 7(6):379–382
99. Ament I et al (2012) Single unlabeled protein detection on individual plasmonic nanoparticles. Nano Lett 12(2):1092–1095
100. Al Balushi AA, Zehtabi-Oskuie A, Gordon R (2013) Observing single protein binding by optical transmission through a double nanohole aperture in a metal film. Biomed Opt Express 4(9):1504–1511
101. Im H et al (2012) Nanohole-based surface plasmon resonance instruments with improved spectral resolution quantify a broad range of antibody-ligand binding kinetics. Anal Chem 84(4):1941–1947
102. Cetin AE et al (2014) Handheld high-throughput plasmonic biosensor using computational on-chip imaging. Light Sci Appl 3:e122
103. Soler M et al (2016) Label-free nanoplasmonic sensing of tumor-associate autoantibodies for early diagnosis of colorectal cancer. Anal Chim Acta 930:31–38
104. Escobedo C et al (2013) Quantification of ovarian cancer markers with integrated microfluidic concentration gradient and imaging nanohole surface plasmon resonance. Analyst 138(5):1450–1458
105. Ruemmele JA et al (2013) A localized surface plasmon resonance imaging instrument for multiplexed biosensing. Anal Chem 85(9):4560–4566
106. Couture M et al (2016) 96-well plasmonic sensing with nanohole arrays. ACS Sensors 1(3):287–294
107. Saha A, Jana NR (2015) Paper-based microfluidic approach for surface-enhanced Raman spectroscopy and highly reproducible detection of proteins beyond picomolar concentration. ACS Appl Mater Interfaces 1:996–1003
108. Chon H et al (2010) On-chip immunoassay using surface-enhanced Raman scattering of hollow gold nanospheres. Anal Chem 82(12):5290–5295
109. Hwang H et al (2010) Optoelectrofluidic sandwich immunoassays for detection of human tumor marker using surface-enhanced raman scattering. Anal Chem 82(18):7603–7610
110. Lee M et al (2011) Highly reproducible immunoassay of cancer markers on a gold-patterned microarray chip using surface-enhanced Raman scattering imaging. Biosens Bioelectron 26(5):2135–2141
111. Zou K et al (2016) Picomolar detection of carcinoembryonic antigen in whole blood using microfluidics and surface-enhanced Raman spectroscopy. Electrophoresis 37(5–6):786–789
112. Kaminska A et al (2015) Detection of hepatitis B virus antigen from human blood: SERS immunoassay in a microfluidic system. Biosens Bioelectron 66:461–467

113. Yanik AA et al (2010) An optofluidic nanoplasmonic biosensor for direct detection of live viruses from biological media. Nano Lett 10(12):4962–4969
114. Walter A et al (2011) Towards a fast, high specific and reliable discrimination of bacteria on strain level by means of SERS in a microfluidic device. Lab Chip 11(6):1013–1021
115. Tokel O et al (2015) Portable microfluidic integrated plasmonic platform for pathogen detection. Sci Rep 5:9152
116. Andreou C et al (2013) Rapid detection of drugs of abuse in saliva using surface enhanced Raman spectroscopy and microfluidics. ACS Nano 7(8):7157–7164
117. Inci F et al (2013) Nanoplasmonic quantitative detection of intact viruses from unprocessed whole blood. ACS Nano 7(6):4733–4745
118. Wang S et al (2012) Portable microfluidic chip for detection of *Escherichia coli* in produce and blood. Int J Nanomedicine 7:2591–2600
119. Durmus NG et al (2013) Fructose enhanced reduction of bacterial growth on nanorough surfaces. MRS Proc 1498:73–78
120. Tasoglu S et al (2013) Manipulating biological agents and cells in micro-scale volumes for applications in medicine. Chem Soc Rev 42(13):5788–5808
121. Wang S et al (2010) Label-free imaging, detection, and mass measurement of single viruses by surface plasmon resonance. Proc Natl Acad Sci 107(37):16028–16032
122. Florschütz K et al (2013) 'Phytochip': on-chip detection of phytopathogenic RNA viruses by a new surface plasmon resonance platform. J Virol Methods 189(1):80–86
123. Srivastava SK et al (2015) Highly sensitive and specific detection of E. Coli by a SERS nanobiosensor chip utilizing metallic nanosculptured thin films. Analyst 140(9):3201–3209
124. Olaru A et al (2015) Surface plasmon resonance (SPR) biosensors in pharmaceutical analysis. Crit Rev Anal Chem 45(2):97–105
125. Chen S et al (2012) Visualization of high-throughput and label-free antibody-polypeptide binding for drug screening based on microarrays and surface plasmon resonance imaging. J Biomed Opt 17(1):0150051–0150058
126. Izake EL (2007) Chiral discrimination and enantioselective analysis of drugs: an overview. J Pharm Sci 96(7):1659–1676
127. Guo L et al (2012) Enantioselective analysis of melagatran via an LSPR biosensor integrated with a microfluidic chip. Lab Chip 12(20):3901–3906
128. Wu Z, Zheng YB (2017) Moiré chiral metamaterials. Adv Opt Mater 5. (in Press)
129. Narsaiah K et al (2012) Optical biosensors for food quality and safety assurance – a review. J Food Sci Technol 49(4):383–406
130. Fernandez F et al (2010) A label-free and portable multichannel surface plasmon resonance immunosensor for on site analysis of antibiotics in milk samples. Biosens Bioelectron 26(4):1231–1238
131. Zhao SS et al (2015) Miniature multi-channel SPR instrument for methotrexate monitoring in clinical samples. Biosens Bioelectron 64:664–670